EUROPEAN ORGANIZATION FOR NUCLEAR RESEARCH

CERN-EP/79-139
12 November 1979

A MODEL-INDEPENDENT PARTIAL WAVE ANALYSIS OF THE REACTION $\pi^- p \to K^+K^- n$ AT $\sim$ 18 GeV/c

CERN-Cracow-Munich Collaboration

L. Görlich, B. Niczyporuk, M. Rózańska, K. Rybicki and J. Turnau

Institute of Nuclear Physics, Cracow, Poland

H. Becker*), G. Blanar, W. Blum, H. Dietl, J. Gallivan, B. Gottschalk**), E. Lorenz, G. Lütjens, G. Lutz, W. Männer, D. Notz***), R. Richter, U. Stierlin and B. Stringfellow†)

Max Planck Institute, Munich, Germany

V. Chabaud, B. Hyams and T. Papadopoulou††)

CERN, Geneva, Switzerland

J. De Groot†††)

Zeeman Laboratory, Amsterdam, The Netherlands

(Submitted to Nuclear Physics B)

*) Now at Technische Fachhochschule, Saarbrücken, Germany.

**) Visitor from Northeastern University, Boston, Mass., USA.

***) Now at DESY, Hamburg, Germany.

†) Now at the Nuclear Research Centre, Strasbourg, France.

††) Now at the National Technical University, Athens, Greece.

†††) Now at CERN, Geneva, Switzerland.

ABSTRACT

The reaction $\pi^- p \to K^+K^- n$ has been studied on a hydrogen target (27,000 events) at 18.4 GeV/c and on a polarized target (54,000 events) at 17.2 GeV/c. A combination of results of both experiments allows a partial-wave analysis of the K^+K^- system between 1.1 and 1.74 GeV mass without any model assumptions. In general our fits yield unique solutions. Using results of our previous analysis of $\pi^+\pi^-$ final states, the branching ratios $BR(\bar{K}K/\pi\pi)$ of partial waves into $\bar{K}K$ and $\pi\pi$ are determined. The S wave appears to be mainly a broad $\varepsilon(1300)$ with $BR(\bar{K}K/\pi\pi) = 0.068^{+0.017}_{-0.021}$. The weak P wave can be described by a tail of the $\rho(770)$ with $BR(\bar{K}K/\pi\pi) = 0.081^{+0.029}_{-0.025}$. The D wave is interpreted in terms of a superposition of $f(1270) + A_2(1310) + f'(1515)$ resonances. The fit yields $BR(\bar{K}K/\pi\pi) = 0.069^{+0.023}_{-0.031}$ for the f(1270) and $BR(\pi\pi/all) = (2.7^{+7.1}_{-1.3})\%$ for the f'(1515). The F wave shows the g(1690) meson with $BR(\bar{K}K/\pi\pi) = 0.191^{+0.040}_{-0.037}$. All the above values refer to the t bin between 0.01 $(GeV/c)^2$ and 0.20 $(GeV/c)^2$. Some results are also given for the high-t region.

1. INTRODUCTION

The K^+K^- system produced in the reaction $\pi^-p \to K^+K^-n$ is intrinsically more complicated than the $\pi^+\pi^-$ system in the reaction $\pi^-p \to \pi^+\pi^-n$, owing to the absence of a G-parity requirement. The allowed natural spin parity states, i.e. $J^P = 0^+, 1^-, 2^+, 3^-, \ldots$, can be produced with isospin I = 0 and I = 1. Their G-parity is $G = (-1)^{J+I}$. Therefore contributions from the resonances listed in Table 1 are expected in the K^+K^- system up to a mass of 1740 MeV.

The negative G-parity resonances, e.g. $\delta(980)$, $\phi(1020)$, $A_2(1310)$ and $\omega(1670)$, do not couple strongly to the $\pi^+\pi^-$ channel. Therefore they cannot be produced by one-pion-exchange (OPE), which is a dominant production mechanism in π-induced reactions at least at low four-momentum transfer t. On the other hand, they can be produced by other exchanges relatively stronger at high t. OPE production of f'(1515) is suppressed by the Okubo-Zweig-Iizuka rule.

The K^+K^- system was extensively investigated by the Effective Mass Spectrometer group [1-4] at Argonne. They studied 110,000 events of the reaction

$$\pi^-p \to K^+K^-n \tag{1}$$

and 50,000 events of the reaction

$$\pi^+n \to K^+K^-p \tag{2}$$

at 6 GeV/c. A simultaneous analysis of both reactions allowed for a decomposition of the K^+K^- system into its I = 0 and I = 1 components. Nevertheless, the number of observables was still too small for a model-independent analysis. Therefore the Argonne group assumed an OPE model with absorption similar to some studies [5-7] of the reaction

$$\pi^-p \to \pi^+\pi^-n\ . \tag{3}$$

Specifically these assumptions were the following:

i) the helicity m = 0 amplitudes are of s-channel spin-flip type,

ii) the unnatural spin-parity exchange (UPE) amplitudes with m = 1 arise from absorption of the dominant m = 0 amplitudes,

iii) the phase between these two amplitudes at the same spin J is either 0° or 180° (phase coherence assumption),

iv) the moduli of natural spin-parity exchange (NPE) and unnatural spin-parity exchange (UPE) amplitudes with helicity m = 1 are equal for a given spin J.

The last assumption was motivated by the vanishing of the relevant $M \geq 2$ moments of the angular distribution for low four-momentum transfer $|t| < 0.08$ $(GeV/c)^2$. Using the above assumptions, the Argonne group performed an energy-independent partial-wave analysis up to ∿ 1600 MeV. The main results [4] were:

The intensity of the D_0 wave rises rapidly up to 1300 MeV, then falls down more slowly. This intensity has not been investigated any further. Instead the t_0^4 moment for $0.08 < |t| < 0.40$ $(GeV/c)^2$ [3] was interpreted in terms of a superposition of f(1270) + A_2(1310) + f'(1515) resonances. This yielded the parameters of the f'(1515) resonance and the f(1270) branching ratio into $\bar{K}K$. A similar analysis of the t_0^4 moment of our data is described elsewhere [8].

There are two solutions peaking at ∿ 1300 MeV either in the S or the P wave. Combining the results for reactions (1) and (2), the S and P waves were decomposed into I = 0 and I = 1 components. Counting phase ambiguities, eight mathematically allowed solutions were found. The solution with the larger I = 0 S wave was favoured by several physical arguments. They were: agreement with the OPE dominance, consistency of the I = 1 P wave with a tail of the ρ(770) resonance, and proper description of the t_0^2 moments in the reaction

$$\pi^- p \rightarrow K_S^0 K_S^0 n \ . \qquad (4)$$

Thus the Argonne group concluded, contrary to some earlier studies [9] of reaction (4), that the S-wave enhancement at ∿ 1300 MeV was an I = 0 and not I = 1 effect. This would be essentially similar to ε(1300) seen in reaction (3); however, its substantial coupling to the K^+K^- channel could be inconsistent with the large elasticity of this object observed in the $\pi^+\pi^-$ studies [5-7].

Recently the Durham-Geneva Collaboration has reported a series of investigations of the reaction

$$\pi^- p \rightarrow K^- K_S^0 p \qquad (5)$$

at 10 GeV/c [10-12]. Studying a pure I = 1 channel, they have observed, in addition to a very strong $A_2(1310)$ and g(1690) resonances, an enhancement in the S wave around 1300 MeV in their favoured solution. This effect, observed for $0.07 < |t| < 1.0\ (GeV/c)^2$, has again complicated the picture of the S wave in the K^+K^- channel.

In this paper the results of a partial-wave analysis of the K^+K^- system, produced peripherally in the reaction $\pi^-p \to K^+K^-n$, are presented. This is based on two experiments performed by the CERN-Munich group in 1973-75. The first has yielded 27,000 events on a hydrogen target at 18.4 GeV/c. The apparatus and data processing are described elsewhere [13,14]. The second experiment has used a polarized (butanol C_4H_9OH) target at 17.2 GeV/c. The apparatus and details of the analysis are described in other works [15,16]. In addition to ∿ 1,200,000 events of the reaction $\pi^-p \to \pi^+\pi^-n$, 54,000 events of the reaction $\pi^-p \to K^+K^-n$ have also been recorded. The additional selection and processing of the K^+K^- events were performed analogously to that in ref. [14].

Only ∿ ⅓ of the K^+K^- events in the polarized-target experiment originate from collisions with free protons. Only these events can contribute to the polarization-dependent part of the angular distribution (average free proton polarization P = 68%). Combining this polarization-dependent part with a polarization-independent part of the angular distribution from the earlier hydrogen experiment, one has enough observables for a model-independent partial-wave analysis without any assumptions on the production mechanism.

This paper is organized as follows. In section 2 the kinematic variables, moments of the angular distribution, partial-wave amplitudes, and fits are described. This description closely follows our analysis of the $\pi^+\pi^-$ system given elsewhere [16-18]. In section 3 resonances and their branching ratios into $\bar{K}K$ and $\pi\pi$ are discussed. Section 4 is devoted to a non-OPE contribution to reaction (1). Section 5 deals with the relative phases of partial waves and the Barrelet zeros of the $\pi\pi \to \bar{K}K$ amplitude. All these results have been obtained at low four-momentum transfer $[0.01 < |t| < 0.20\ (GeV/c)^2]$. In section 6 some results at high t $[0.2 < |t| < 1.0\ (\mathrm{GeV}/c)^2]$ are also shown. Some concluding remarks are given in section 7.

2. VARIABLES, MOMENTS, AMPLITUDES AND FITS

At a given energy the reaction $\pi^- p \to K^+K^- n$ can be described by the following five variables (see refs. [16-18] for figures showing the ψ, θ, and ϕ angles):

m_{KK}: effective mass of the K^+K^- system,

t : square of four-momentum transfer of the initial proton to the final neutron,

ψ : polarization angle (the angle between the normal to the reaction plane and the polarization direction),

$\left.\begin{matrix}\theta\\ \phi\end{matrix}\right\}$: decay angles of the K^- in the K^+K^- rest system. [the Gottfried-Jackson reference system (i.e. t-channel) has been used].

Owing to parity conservation and spin ½ of the nucleon, the general form of the angular distribution for the reaction (1) is the following:

$$W(\theta,\phi,\psi,m_{KK},t) = \sum_{L,M} t^L_M(m_{KK},t)\ \mathrm{Re}\ Y^L_M(\cos\theta,\phi) + P\cos\psi \sum_{L,M} p^L_M(m_{KK},t)\ \mathrm{Re}\ Y^L_M(\cos\theta,\phi) + P\sin\psi \sum_{L,M} r^L_M(m_{KK},t)\ \mathrm{Im}\ Y^L_M(\cos\theta,\phi)\ ,$$

where

P is the polarization perpendicular to the beam direction,

$Y^L_M(\cos\theta,\phi)$ are the spherical harmonic functions.

The normalized moments t^L_M, p^L_M and r^L_M of the angular distribution are defined as:

$$t^L_M = \varepsilon_M\left\langle \mathrm{Re}\ Y^L_M(\cos\theta,\phi)\right\rangle = \frac{\varepsilon_M}{2\pi}\iiint W(\theta,\phi,\psi)\ \mathrm{Re}\ Y^L_M(\cos\theta,\phi)\ d\cos\theta\ d\phi\ d\psi$$

$$p^L_M = 2\varepsilon_M\left\langle \mathrm{Re}\ Y^L_M(\cos\theta,\phi)\cos\psi\right\rangle = \frac{\varepsilon_M}{\pi}\iiint W(\theta,\phi,\psi)\ \mathrm{Re}\ Y^L_M(\cos\theta,\phi)\cos\psi\ d\cos\theta\ d\phi\ d\psi$$

$$r^L_M = 4\left\langle \mathrm{Im}\ Y^L_M(\cos\theta,\phi)\sin\psi\right\rangle = \frac{2}{\pi}\iiint W(\theta,\phi,\psi)\ \mathrm{Im}\ Y^L_M(\cos\theta,\phi)\sin\psi\ d\cos\theta\ d\phi\ d\psi\ ,$$

where $\varepsilon_{M=0} = 1$, $\varepsilon_{M\neq 0} = 2$.

For our partial-wave analysis the t_M^L moments from the hydrogen-target experiment [13,14] at 18.4 GeV/c are combined with the p_M^L and r_M^L moments from the polarized-target experiment at 17.2 GeV/c. The difference in the primary momentum has been corrected by assuming a p_{lab}^{-2} dependence of the cross-section for the reaction $\pi^- p \to K^+K^- n$.

Figure 1 shows the mass dependence of the t-channel moments for $0.01 < |t| < 0.20$ (GeV/c)^2. The upper limit of 1740 MeV of the K^+K^- effective mass in our analysis is motivated by the fact that the h(2040) resonance in the G wave is expected to be important above this mass. The lower limit of four-momentum transfer of $|t| < 0.01$ (GeV/c)^2 has been chosen to be above the kinematic limit at m_{KK} = 1740 MeV. The upper limit has been set at 0.20 (GeV/c)^2, because there is no strong t-dependence of the normalized moments below this value. Therefore a single t-bin analysis is performed instead of an extrapolation to the π pole. The t and the mass binning Δm_{KK} = 40 MeV is identical to that in ref. [17], thus allowing an easy comparison with $\pi^+\pi^-$ results. The following conclusions can be drawn from fig. 1.

i) The mass distribution exhibits a broad peak centred at 1350 MeV and a smaller one around 1700 MeV. An inspection of the t_M^L moments immediately shows that these are D and F wave effects, respectively.

ii) The absolute values of the p_0^0 and p_0^2 are smaller than those for the $\pi^+\pi^-$ channel, shown as continuous lines in the figures. This indicates a difference in the production mechanisms at least below $\sim$ 1400 MeV.

iii) The r_M^L moments are small; thus contributions from NPE must be small.

iv) All $M \geq 2$ moments are consistent with zero. Therefore all $m > 1$ amplitudes are neglected in our analysis. Contrary to the analysis of the Argonne group, identical vanishing of M = 2 moments has not been assumed. This enables us to extend our analysis to high four-momentum transfer using the same formulae and programs (see section 6).

For the following analysis we will use the nucleon transversity amplitudes. The moments are related to the nucleon transversity (spin component perpendicular to the reaction plane) amplitudes by the following formulae (explicitly derived in ref. [18]):

$$t^L_M = \sum_{j,k} c^{LM}_{jk} \, \mathrm{Re} \left({}^U g_j {}^U g^*_k + {}^U h_j {}^U h^*_k + {}^N g_j {}^N g^*_k + {}^N h_j {}^N h^*_k \right)$$

$$p^L_M = \sum_{j,k} c^{LM}_{jk} \, \mathrm{Re} \left({}^U g_j {}^U g^*_k - {}^U h_j {}^U h^*_k - {}^N g_j {}^N g^*_k + {}^N h_j {}^N h^*_k \right)$$

$$r^L_M = \sum_{j,k} c^{LM}_{jk} \, \mathrm{Re} \left(-{}^U g_j {}^N g^*_k + {}^U h_j {}^N h^*_k + {}^N g_j {}^U g^*_k - {}^N h_j {}^U h^*_k \right) ,$$

where

U(N) denotes unnatural (natural) spin-parity exchange,

j or k stands for the K^+K^- spin ℓ and helicity m indices,

c^{LM}_{jk} contains the Clebsch-Gordan coefficients, etc.,

g(h) stands for amplitude with nucleon transversity down (up).

An advantage of nucleon transversity amplitudes (hereafter referred to as transversity amplitudes) is the possibility of determining them without any model assumptions from our data. More exactly, one can find all amplitudes for a given transversity of g or h, but the phase between these two sets of amplitudes remains unknown. For the determination of this phase, a measurement of the recoil polarization would be necessary (see ref. [18]). However, even without this phase, one can calculate $|g^\ell_m|^2 + |h^\ell_m|^2$, the intensity of the partial wave characterized by the K^+K^- spin ℓ and helicity m.

The transversity amplitudes are related to the helicity amplitudes by the following formulae:

$$\left.\begin{aligned} {}^U g^\ell_m &= \frac{1}{\sqrt{2}} \left({}^U n^\ell_m + i \, {}^U f^\ell_m \right) \\ {}^N g^\ell_m &= \frac{1}{\sqrt{2}} \left({}^N n^\ell_m - i \, {}^N f^\ell_m \right) \end{aligned}\right\} \text{recoil transversity down}$$

$$\left.\begin{aligned} {}^U h^\ell_m &= \frac{1}{\sqrt{2}} \left({}^U n^\ell_m - i \, {}^U f^\ell_m \right) \\ {}^N h^\ell_m &= \frac{1}{\sqrt{2}} \left({}^N n^\ell_m + i \, {}^N f^\ell_m \right) \end{aligned}\right\} \text{recoil transversity up}$$

where n_m^ℓ and f_m^ℓ are helicity amplitudes corresponding to nucleon spin non-flip and flip, respectively.

For s-channel nucleon helicities the n_m^ℓ amplitudes are zero for pure OPE, for any ℓ,m. In the language of transversity amplitudes this corresponds to $|{}^U g_m^\ell| = |{}^U h_m^\ell|$. In this case, the p_M^L and r_M^L moments should vanish almost identically. Although these moments are indeed very small, the ${}^U g_m^\ell$ and ${}^U h_m^\ell$ amplitudes are still left free in our fits. The reason is that within errors of the p_M^L and r_M^L moments there still might be a considerable difference between the g and h amplitudes. This will be discussed in sections 4 and 7.

Determination of the transversity amplitudes from the t-channel moments exactly follows our analysis of the $\pi^+\pi^-$ system described in refs. [16,17]. The whole mass interval has been divided into two regions of 1100-1460 and 1460-1740 MeV. The mass region below 1100 MeV has been excluded from our analysis owing to experimental difficulties. Below 1460 MeV the F wave can be neglected. This has been checked by performing fits with and without this wave. Below 1740 MeV the G wave (ℓ = 4) is not taken into account. The characteristics of both regions are given in table 2.

We perform an energy-independent analysis, i.e. each mass bin is fitted separately with many starting values independently of neighbouring bins. The starting values are either several sets of random quantities or analytical solutions of a simplified version of the equation system relating moments to amplitudes (see refs. [17 and 18] for details). In addition, once a solution is reached, the method of Barrelet zeros [19] is used to search for other solutions.

The fits are good and usually yield a unique solution or two solutions with overlapping errors. The results are presented in the following section; the problem of ambiguities will be discussed in section 5.

3. INTENSITIES OF PARTIAL WAVES

As has already been mentioned, the intensities of partial waves can be calculated as

$$|S|^2 = \frac{d^2\sigma}{dtdm_{KK}} (|g_0^0|^2 + |h_0^0|^2)$$

$$|P_0|^2 = \frac{d^2\sigma}{dtdm_{KK}} (|g_0^1|^2 + |h_0^1|^2)$$

$$|P_U|^2 = \frac{d^2\sigma}{dtdm_{KK}} (|{}^Ug_1^1|^2 + |{}^Uh_1^1|^2)$$

$$|P_N|^2 = \frac{d^2\sigma}{dtdm_{KK}} (|{}^Ng_1^1|^2 + |{}^Nh_1^1|^2) \text{ , etc. .}$$

The errors of the cross-section per event in each experiment ($\sim$ 5%) have been included in the errors of our intensities. These intensities are shown in fig. 2 in units of microbarns per 40 MeV mass bins.

Before proceeding with the description of the dominant m = 0 waves, let us make some remarks on the branching ratios into $\bar{K}K$ and $\pi\pi$. Except for the f′, their calculation is based on a direct comparison of the K^+K^- intensities with the $\pi^+\pi^-$ intensities determined in ref. [17]. Since both partial-wave intensities have been determined from experiments performed with basically the same apparatus and analysed in the same way, systematic errors will cancel out. The only assumption made here is that on the same production mechanism in reaction $\pi^-p \to K^+K^-n$ and reaction $\pi^-p \to \pi^+\pi^-n$. Both reactions are assumed to be dominated by OPE with a small admixture of other exchanges. This admixture is different for the two reactions, as odd G-parity states are allowed in the K^+K^- system. The branching ratios are calculated, neglecting the difference in the admixture. The quality of this assumption will be discussed for each partial wave separately. The experimental values of branching ratios are compared [20,21] in table 3 with the quark-model calculations of Feynman, Kislinger and Ravndall [21]. Their model assumes a four-dimensional harmonic oscillator potential for the mass squared operator and uses phenomenological parameters and formulae.

3.1 The S wave

Our S-wave solution exhibits an enhancement around 1300 MeV, similar to that observed by the Argonne group [4]. However, their S-wave solution is nearly as strong as the D_0 wave, while ours is much weaker. The difference may be partially attributed to the m = 1 amplitudes (P_U,P_N,D_U,D_N). The Argonne group has explicitly assumed the absorption-model relations between $P_U(D_U)$ and $P_0(D_0)$ amplitudes as well as $|P_U| = |P_N|$, $|D_U| = |D_N|$ equalities. On the other hand, in our fits, all m = 1 waves have been left free. As will be seen in the next section, the m = 1 P-wave intensities obtained in our fit are stronger than the absorption-model predictions, probably at the expense of the S wave. This effect cannot, however, account for the whole difference, even if the full P_U and P_N intensities are added to that of the S wave. Moreover, the absorption-model constraint would reduce the P_U, and consequently the P_N intensities, but would increase the P_0 one. Therefore a possible net effect on the S wave would be even smaller.

In the mass region from 1100 MeV to 1500 MeV, the shape of the S-wave enhancement is fairly similar to that in the $\pi^+\pi^-$ S wave of ref. [17]. Therefore we tend to follow the conclusion of the Argonne group [4] that the K^+K^- S wave is mainly an I = 0 state. This seems to contradict a recent partial-wave analysis by Martin et al. [10,12] of the reaction $\pi^-p \rightarrow K^-K^0_Sp$, a pure I = 1 state. The S-wave enhancement at 1250 MeV in their favoured solution is stronger than the $A_2(1310)$ resonance in the D_0 wave by at least a factor of 2.

However, the CERN-Munich results [22,23] at 9.8 GeV/c, 12.7 GeV/c and 18.8 GeV/c show that the $A_2(1310)$ production dominates the reaction $\pi^\pm p \rightarrow K^\pm K^0_S p$. The total background, including a possible S wave, amounts to only (10-15%) of the cross-section.

Assuming that the S-wave enhancement is mainly an I = 0 ε state, the branching ratio $BR(\bar{K}K/\pi\pi) = 0.068^{+0.017}_{-0.021}$ has been obtained. Further, assuming absence of any other decay channels, one can calculate $x(\varepsilon \rightarrow \bar{K}K) = (6.4^{+1.6}_{-2.0})\%$, where x denotes the partial branching ratio for a given channel. Contrary to the Argonne results [4], the S wave can still be reconciled with a high elasticity of the $\varepsilon(1300)$ known from $\pi\pi$ studies [6,7]. Thus the K^+K^- S-wave enhancement can be interpreted as being mainly the $\varepsilon(1300)$.

The FKR model [20,21] predicts a branching ratio of $x(\varepsilon \rightarrow \bar{K}K) = 0.237$, substantially higher than our result. This discrepancy, contrasting with the good agreement for the f(1270) and g(1690) resonances, might be due to the fact that the FKR model is sometimes wrong in details, while giving a correct over-all picture as discussed by Hey and Morgan [21].

3.2 The P_0 wave

The P_0 wave is relatively weak in the entire mass range. It is probably in a fairly pure I = 1 state. From the simultaneous study of reactions (1) and (2), the Argonne group [4] has concluded that the I = 0 P_0 wave intensity is at least an order of magnitude lower than the I = 1 one, as expected by OPE dominance. The I = 1 state can be associated with the tail of the ρ(770) resonance. Following this assumption, we have determined the ρ(770) branching ratio. In order to compare our result with the SU(3) prediction, we separated out the kinematical factors for each mass bin calculating:

$$\left(\frac{g_{\rho\to K^+K^-}}{g_{\rho\to\pi^+\pi^-}}\right)^2 = \frac{|P_0(K^+K^-)|^2}{|P_0(\pi^+\pi^-)|}\left(\frac{q_\pi}{q_K}\right)^3 \frac{D_1(q_K r)}{D_1(q_\pi r)} ,$$

where

g_ρ is a ρ coupling constant to the $\bar{K}K$ or ππ channel,

q_π (q_K) is a decay π (K) momentum in the ππ ($K\bar{K}$) rest system,

$D_1(qr) = 1 + (qr)^2$,

r = 1 fm.

The average $0.051\,^{+\,0.051}_{-\,0.038}$ is clearly smaller than the SU(3) prediction of ¼. Without the centrifugal barrier functions D(qr), as in ref. [12], we obtain the value of $0.109\,^{+\,0.105}_{-\,0.079}$ still below the SU(3) prediction.

3.3 The D_0 wave

Our D_0-wave solution exhibits a broad enhancement between 1200 MeV and 1500 MeV. The enhancement cannot be described by a single resonance. Such an attempt leads to $\chi^2/NDF = 24.9/10$ and yields a mass = (1331 ± 9) MeV and width = $(165\,^{+\,16}_{-\,14})$ MeV. Fixing this resonance to be the f(1270) yields an even larger value of $\chi^2/NDF = 55.2/13$. Therefore, as in refs. [3,8], the D_0 wave is described by a superposition of 3 possible resonances, i.e f(1270), A_2(1310) and f′(1515). Thus the D_0 intensity has been fitted by the following formula:

$$|D_0|^2 = \frac{m_{KK}^2}{q_\pi}\left|\alpha_f^{KK}\frac{BW_f(m_{KK})}{|BW_f(m_f)|} + \alpha_{A_2}^{KK}\, e^{i\phi_{A_2}}\frac{BW_{A_2}(m_{KK})}{|BW_{A_2}(m_{A_2})|} + \alpha_{f'}^{KK}\, e^{i\phi_{f'}}\frac{BW_{f'}(m_{KK})}{|BW_{f'}(m_{f'})|}\right|^2$$

$$BW_R(m_{KK}) = \frac{m_R\sqrt{\Gamma_{\pi\pi}\Gamma_{KK}}}{m_R^2 - m_{KK}^2 - i\, m_R\Gamma_{tot}} \qquad \text{for } R = f, f'$$

$$BW_R(m_{KK}) = \frac{m_R\sqrt{\Gamma_{KK}\Gamma_R}}{m_R^2 - m_{KK}^2 - i\, m_R\Gamma_{tot}} \qquad \text{for } R = A_2 \;.$$

The Breit-Wigner formula for the A_2 resonance has been taken from the recent studies [22,23] of $A_2^{\pm}$ production in reaction (4) at 9.8, 12.7 and 18.8 GeV/c.

$$\Gamma_{\pi\pi} = \Gamma_R^{\pi\pi}\left(\frac{q_\pi}{q_\pi^R}\right)^5 \frac{D_2(q_\pi^R r)}{D_2(q_\pi r)}$$

$$\Gamma_{KK} = \Gamma_R^{KK}\left(\frac{q_K}{q_K^R}\right)^5 \frac{D_2(q_K^R r)}{D_2(q_K r)}$$

$$\Gamma_{tot} = \Gamma_R\left(\frac{q}{q^R}\right)^5 \frac{D_2(q^R r)}{D_2(qr)} \;,$$

where

q : c.m. momenta of secondary particles in the dominant decay channel of the resonance R - $\pi\pi$ for f, $\rho\pi$ for A_2 and $\bar{K}K$ for f′ [24];

q_π, q_K : c.m. momenta for the $\pi\pi$, KK decay;

q_i^R : c.m. momentum of the decay particle i, at the resonance mass m_R;

Γ_R : resonance width;

$D_2(qr) = 9 + 3(qr)^2 + (qr)^4$;

α_R^{KK} : magnitude of the amplitude at the resonance R position;

ϕ_R : relative production phases with respect to the f resonance.

Obviously our parametrization of the D_0 wave is a simplification, as each resonance in fact consists of two components (e.g. nucleon spin-flip and spin non-flip ones). Our formula corresponds to full nucleon spin coherence. This is based on the assumptions that the f(1270) and f′(1515) are produced by the same production mechanism (OPE) and the A_2(1310) production is small. These assumptions are consistent with the results of our fits.

In our fits the parameters of the f(1270) and A_2(1310) have been fixed at their table values [25] of m_f = 1271 MeV, Γ_f = 180 MeV, m_{A_2} = 1312 MeV, Γ_{A_2} = = 102 MeV, while the contributions α of all amplitudes and their relative phases have been left free. The results of the fits are given in table 4. In fits 1 and 2 the $A_2(1310)$ was allowed, whereas it was neglected in fit 3. In fits 1 and 3 the f′(1515) parameters have been left free, while in fit 2 they were fixed at their table values.

All these fits show that the D_0 is dominated by the f(1270), with a small admixture of the $A_2(1310)$ and a considerable contribution of f′(1515). In further discussions, we will use the results of fit 1 to determine the branching ratios of f(1270) and f′(1515) resonances.

Comparing the magnitude of the amplitude α_f^{KK} in this fit with $\alpha_f^{\pi\pi} = 0.540 \pm$ $\pm\, 0.010$, obtained in a fit of f(1270) to the D_0 wave in reaction $\pi^- p \to \pi^+\pi^- n$, yields the following branching ratio:

$$BR(\bar{K}K/\pi\pi) = \frac{x(f \to \bar{K}K)}{x(f \to \pi\pi)} = \frac{\frac{2}{3}\left(\alpha_f^{KK}\right)^2}{\frac{1}{2}\left(\alpha_f^{\pi\pi}\right)^2} = 0.069 \begin{array}{l} +\,0.023 \\ -\,0.031 \end{array} ,$$

where ½ and ⅔ are isospin factors for the $\bar{K}K$ and $\pi\pi$ systems, respectively. Using $x(f \to \pi\pi) = (84.7 \pm 1.6)\%$ from ref. [17], we obtain $x(f \to \bar{K}K) = (5.8\ ^{+1.9}_{-2.6})\%$. Thus only 10% is left for other decay channels, probably mainly 4π. Another estimate of this branching ratio comes from a direct comparison of the D_0 intensities in both reactions below 1300 MeV, where neither the $A_2(1310)$ nor the f′(1515) would strongly contribute. This comparison yields $BR(\bar{K}K/\pi\pi) = 0.056 \pm 0.006$ consistent with the above value. Both our values agree with $BR(\bar{K}K/\pi\pi) = 0.047 \pm 0.009$ obtained by the Argonne group [4]. While the bubble-chamber experiments (c.f. review in ref. [25]) lead to conflicting results with large errors, the analysis of the reaction $\pi^- p \to K_S^0 K_S^0 n$ by the CERN-ETH collaboration [26,27] yields $BR(\bar{K}K/\pi\pi) =$ $= 0.029 \pm 0.006$, about half of our value. This reduction by approximately a factor of 2 is also observed for the S-wave threshold enhancement when comparing our 18.4 GeV/c data [14] with their data. On the other hand, the recent paper of the Notre Dame group [28] on the reaction $\pi^- p \to K_S^0 K_S^0 n$ yields again the low value of $BR(\bar{K}K/\pi\pi) = 0.027 \pm 0.009$. Our values of $BR(\bar{K}K/\pi\pi)$ are consistent with the value of 0.058 predicted by the FKR quark model.

The fit yields an $f' - f$ relative phase of $(163 \pm 20)°$ consistent with the OPE prediction of 180°. Assuming that the $f'(1515)$ is produced by an OPE production mechanism, the branching ratio $x(f' \to \pi\pi)$ can be determined in the following manner:

From the fit to the D_0 intensity in the reaction $\pi^- p \to K^+K^- n$

$$\left(\frac{\alpha_{f'}^{KK}}{\alpha_f^{KK}}\right)^2 = \frac{x(f' \to \pi\pi)\ x(f' \to \bar{K}K)}{x(f \to \pi\pi)\ x(f \to \bar{K}K)} \ .$$

Substituting $x(f \to \bar{K}K)/(\alpha_f^{KK})^2$ from the previous equation, we obtain

$$x(f' \to \pi\pi)x(f' \to \bar{K}K) = \frac{4}{3}\left(\frac{\alpha_{f'}^{KK}}{\alpha_f^{\pi\pi}}\ x(f \to \pi\pi)\right)^2 \ .$$

Taking $\alpha_{f'}^{KK} = 0.071\ ^{+\ 0.093}_{-\ 0.017}$ and $\alpha_f^{\pi\pi} = 0.540 \pm 0.010$ from our fits, $x(f \to \pi\pi) =$ $= (84.7 \pm 1.6)\%$ from ref. [17] and the SU(3) prediction [29] of $x(f' \to \bar{K}K) = 70\%$, we obtain

$$x(f' \to \pi\pi) = \left(2.7\ ^{+\ 7.1}_{-\ 1.3}\right)\% \ ,$$

where the large positive error reflects the very asymmetric profile of a χ^2 dependence on $\alpha_{f'}^{KK}$. Fits 2 and 3 yield even larger values of $x(f' \to \pi\pi)$, always at the same assumption of OPE production of $f'(1515)$.

The value of $x(f' \to \pi\pi)$ and other parameters of the $f'(1515)$ resonance obtained in our fits are compared in table 5 with those from other works. Three of them were averaged in the last edition of the Particle Data Group [25] review. These are the Amsterdam-CERN-Nijmegen-Oxford experiment [30] on the reaction

$$K^- p \to K_S K_S \Lambda^0 (\Sigma^0) \ , \qquad (6)$$

the Omega experiment [31] on the reaction

$$K^- p \to K^+ K^- \Lambda^0 (\Sigma^0) \ , \qquad (7)$$

and the Argonne analysis [4]. The result of the Birmingham - Rutherford - Tel-Aviv - London Collaboration [32] is also given in table 5. This could be the first direct observation of $f'(1515)$ in the $\pi^+\pi^-$ channel. However, the $x(f' \to \pi\pi)$ value obtained in this model-independent analysis is so large that the authors have been reluctant to identify their D-wave object with the f′(1515) resonance.

The results based on a study of the reaction $\pi^- p \to K^0_S K^0_S n$ [26-28] are also quoted in table 5. Let us remark here that the upper limit for $x(f' \to \pi\pi)$ given by the CERN-ETH Collaboration [26,27] will go up by a factor of 2 if our branching ratios for f(1270) are used. Thus a branching ratio of the order of 2-3% seems to emerge from the controversial values listed in table 5.

Table 5 shows that also the width of the f′(1515) is not yet well established and its true value is probably higher than 65 ± 10 MeV quoted in the last PDG [25] review.

Concluding the discussion of the D_0 wave, let us comment on our results and those of the Argonne group [4]. They are essentially consistent except for the magnitude of errors, ours being much larger. An explanation of this difference is the following. The Argonne group has fitted their unnormalized t^4_0 moment, assuming it to reflect the D_0 intensity plus the tail of the g(1690) resonance. In fact this moment contains contributions from the D_U and D_N intensities, which might but do not have to follow the D_0 pattern exactly, and from the P-F wave interferences. Our solution for the D_0 wave is a result of a fit of all amplitudes to all moments without any assumptions. Therefore the D_0 intensity is free from any contamination from other waves, but its errors are relatively large. These errors are obviously propagated into the errors of resonance parameters.

3.4 The F_0 wave

Our F_0 wave solution, dominating the high-mass region, clearly shows the g(1690) resonance. The branching ratio $BR(\bar{K}K/\pi\pi) = 0.191 ^{+0.040}_{-0.037}$ in the mass range is in perfect agreement with the value of 0.193 ± 0.025 obtained [14,33] by comparing the t^6_0 moments in the reaction $\pi^- p \to K^+K^- n$ and the reaction $\pi^- p \to \pi^+\pi^- n$. Calculating the branching ratio we have neglected a possible I = 0 component. Let us remark here that the $\bar{K}K$ decay of the ω(1670), which is the only known isoscalar resonance in this wave, has not yet been observed and its ϕ partner has not yet been found.

Our value of the branching ratio is clearly larger than $BR(\bar{K}K/\pi\pi) = 0.056 \pm \pm 0.034$ (note a factor of 2 mistakenly omitted in the error calculation) obtained by Martin et al. [12] in reaction (5) at 10 GeV/c. This value has been calculated fitting the Chew-Low form to the t-dependence of their F_0 wave intensity above $|t| = 0.07\ (\mathrm{GeV}/c)^2$. Our estimate is more direct and does not depend on any model.

The SU(3) prediction for $BR(\bar{K}K/\pi\pi) = 0.12$ or 0.32, depending on whether the centrifugal barrier functions $D_3(q^R r)$ are neglected or used.

Taking

$$x(g \to \pi\pi) = \left(25.9 \begin{smallmatrix} + 1.8 \\ - 1.9 \end{smallmatrix}\right)\%$$

from ref. [17], we obtain

$$x(g \to \bar{K}K) = \left(4.9 \begin{smallmatrix} + 1.1 \\ - 1.0 \end{smallmatrix}\right)\% \ .$$

4. A NON-OPE CONTRIBUTION TO THE PRODUCTION MECHANISM

Additional observables supplied by the polarized-target experiment allow us to investigate a possible production mechanism in addition to OPE with absorption. In particular, for the reaction $\pi^- p \to \pi^+\pi^- n$, both a spin non-flip component in the dominant $m = 0$ amplitudes and an excess of $m = 1$ waves compared to absorption-model predictions was determined in refs. [16 and 17]. It is more difficult to find such effects in the reaction $\pi^- p \to K^+K^- n$, since both the statistics and the polarization effects are smaller here.

The $|g_0^\ell|/|h_0^\ell|$ ratio for the two strongest ($\ell = 2$ and $\ell = 3$) waves are shown in fig. 3. For pure OPE one expects $|g_0^\ell| = |h_0^\ell|$. The $\pi^+\pi^-$ D_0 wave in ref. [17] shows a significant deviation from OPE attributed to the presence of a spin non-flip amplitude corresponding to the exchange of an object with the quantum numbers of the A_1 resonance. A lower limit of non-flip/flip ratio has been determined from the formula [16-18]:

$$\left|n_0^D\right|_{min} = \frac{\left|\,|g_0^D| - |h_0^D|\,\right|}{\sqrt{2}}$$

to be $\sim 16\%$ for the f(1270). Since this resonance is also dominantly contributing to the D_0 wave in the reaction $\pi^- p \to K^+K^- n$, a similar effect is expected too. It is seen however in fig. 3 that this effect is considerably weakened, the K^+K^- points falling between the $\pi^+\pi^-$ results and the $|g_0^D| = |h_0^D|$ line. Consequently, the average value of a lower limit of non-flip/flip ratio of 6-9% is only half of the above value for the reaction $\pi^- p \to \pi^+\pi^- n$. The difference is probably due to a particular $A_2(1310)$ production mechanism at least partially cancelling the A_1 exchange effect in the f(1270) production. This will be discussed more quantitatively in ref. [8].

The F_0 wave in both channels does not show any significant deviation from OPE as the $|g_0^F|/|h_0^F|$ ratio fluctuates around unity. The same is true for the D_0 wave at high mass. Thus non-OPE mechanisms become relatively less important above $\sim$ 1500 MeV.

A similar tendency can be observed for the m = 1 amplitudes. As shown in fig. 2, they are weak but significant. The relations $|P_U| = |P_N|$, $|D_U| = |D_N|$ and $|F_U| = |F_N|$ are at least approximately satisfied. In section 6 it will be seen that the NPE amplitudes become relatively larger at high four-momentum transfer. The UPE m = 1 amplitudes were usually interpreted in terms of an absorption of the dominant m = 0 OPE amplitudes. The "Poor Man's Absorption Model" of Williams [34] predicts the following relation:

$$\frac{|P_U|}{\sqrt{2}\ |P_0|} = \frac{|D_U|}{\sqrt{6}\ |D_0|} = \frac{|F_U|}{\sqrt{12}\ |F_0|} = \frac{c_A}{m_{KK}} ,$$

where c_A represents the strength of absorption. It has been found in reaction (1) that c_A slowly decreases with increasing mass.

The ratios for the K^+K^- amplitudes are shown in fig. 4. The relation between m = 1 and m = 0 UPE amplitudes used by the Argonne group [4] roughly corresponds to our $|D_U|/(\sqrt{6}|D_0|)$ points. While these and the F-wave points follow the trend of the $\pi^+\pi^-$ data, the P-wave points are systematically higher. We do not see any explanation for the high $|P_U|/|P_0|$ ratio, in particular for the apparent enhancement around 1200 MeV in the P_U and P_N waves. However the P wave is our weakest and the worst determined wave. For the well-determined D and F waves the ratios $|D_U|/|D_0|$ and $|F_U|/|F_0|$ are slowly decreasing with increasing mass as in the $\pi^+\pi^-$ channel [17], though their values are generally higher.

5. RELATIVE PHASES AND BARRELET ZEROS OF TRANSVERSITY AMPLITUDES

All relations between moments and amplitudes involve the cosines of the relative phases. Therefore our results have a sign ambiguity, i.e. all the relative phases for a given transversity can be simultaneously multiplied by (-1). In fig. 5 the version most similar to the $\pi^+\pi^-$ data is plotted, i.e. assuming that the P_0-D_0 phase is positive. It should be remembered that the phases between the transversity amplitudes are not necessarily equal to those between the relevant helicity amplitudes. As shown in refs. [16,17], in order to have this equality it is necessary, for example, that the phase between any g amplitudes is equal to the phase between the relevant h amplitudes. The main features of the relative phases are shown in fig. 5. The g and h relative phases show some differences, but large errors prevent us from concluding a definite discrepancy.

The P_0-D_0 phase falls down from $\sim$ 110° at 1150 MeV to $\sim$ 30° at 1400 MeV. This is roughly what can be expected for the D_0 wave rising through f(1270) and other resonances, while the P_0 phase is relatively stable at the value of 140°-150°. The $\pi^+\pi^-$ phase shift studies [35] favour this value over that of 170° assumed by the Argonne group in ref. [4].

The S_0-D_0 phase is very similar to that fitted by the CERN-ETH Collaboration [26,27]. Their result indicates a slow change of the S phase as is expected for a broad ε(1300). Contrary to the $\pi^+\pi^-$ results the relative phase is fairly large.

Finally our results on the D_U-D_0 phase represent a test of the phase coherence assumption. This appears to be only approximately satisfied, as many points deviate from 180°.

The relative phases at higher mass generally follow the trend of the $\pi^+\pi^-$ results [17]. Owing to low statistics, however, they are not too meaningful. For detailed results the reader is referred to another work [36].

Before discussing the Barrelet zeros of the K^+K^- transversity amplitudes, let us note the basic formulae. The $\pi\pi \to \bar{K}K$ amplitude for each transversity can be written as follows (for $\ell_{max} = 3$):

$$A(m_{KK}, z = \cos\theta) = S(m_{KK}) + \sqrt{3}P_0(m_{KK})z + \sqrt{5}D_0(m_{KK})\left(\frac{3}{2}z^2 - \frac{1}{2}\right) + \sqrt{7}F_0(m_{KK})\left(\frac{5}{2}z^3 - \frac{1}{2}z\right) =$$

$$= c \prod_{i=1}^{3} (z - z_i) \, ,$$

where c and z_i are complex functions of m_{KK}. Only the modulus of the amplitude is an observable, i.e.

$$\frac{d^2\sigma(\pi\pi \to \bar{K}K)}{dm_{KK}dt} \propto |A(m_{KK}, z)|^2 = |c|^2 \prod_{i=1}^{3} \left[(z - z_i)(z - z_i^*)\right] =$$

$$= |c|^2 \prod_{i=1}^{3} \left[(z - \text{Re } z_i)^2 + |\text{Im } z_i|^2\right] .$$

The observable is invariant under $z_i \rightleftarrows z_i^*$. A standard method of finding new solutions for amplitudes is to calculate the Barrelet zeros for any reasonable fit, then to flip the signs of their imaginary parts, calculate the new partial waves and finally use them as the starting values for the amplitude-fitting program. A need for refitting comes from the non-OPE contribution. Thus one would expect many ambiguities; fortunately, each new zero enters the physical region with the negative imaginary part; thus Im $z_2 < 0$ below f(1270) and Im $z_3 < 0$ below g(1690). The Barrelet zeros are usually numbered according to the increasing real part, i.e. Re z_1 < Re z_2 < Re z_3.

In fig. 6 the Barrelet zeros for the K^+K^- transversity amplitudes are compared to the $\pi^+\pi^-$ ones from ref. [17]. It is immediately seen that Im z_1 fluctuates around zero and the z_1 cannot produce any ambiguities. This is the zero yielding the main ambiguities in previous studies, i.e. two solutions differing in the S and P waves above 1200 MeV in reaction $\pi^-p \to K^+K^-n$ (see ref. [4]), reaction $\pi^-p \to \pi^+\pi^-n$ (see refs. [6] and [7]), and reaction $\pi^-p \to K^-K^0_S p$ (see refs. [10-12]). In this mass region only one solution has been found in our analysis, though various starting points have been used for the fit. Below $\sim$ 1400 MeV we find Im $z_2 < 0$ as expected for a new zero. Above 1500 MeV |Im z_2| becomes significant again, contrary to the $\pi^+\pi^-$ results, so one might expect an ambiguity in this mass region. However, our fits have gone back to the original values. This is slightly surprising, since an ambiguity-breaking non-OPE contribution is not strong here. Im z_3 is negative below 1600 MeV, but then z_3 is purely real and produces no ambiguities.

Except for the second zero above 1500 MeV, the $\pi^+\pi^- \to K^+K^-$ cross-section vanishes in its minima like the $\pi^+\pi^- \to \pi^+\pi^-$ one. The positions of the minima, however, considerably differ in both reactions, as can be seen from the behaviour of Re z_i in fig. 6.

6. PARTIAL WAVES AT HIGH FOUR-MOMENTUM TRANSFER

The main features of partial waves at high four-momentum transfer of $0.2 < |t| < 1.0\ (\mathrm{GeV/c})^2$ are briefly discussed. The results obtained by integration over such a large t bin should be treated with some caution, since there is a considerable change of the normalized moments between $|t| = 0.2\ (\mathrm{GeV/c})^2$ and $|t| = 1.0\ (\mathrm{GeV/c})^2$. Nevertheless, it is interesting to obtain some information on this poorly known region far from the pion pole.

The moments in this t bin are shown in fig. 7. The M = 2 moments are fairly large. Since their vanishing has not been assumed in our fits, the same amplitude-fitting programs can be used provided M ≥ 3 moments are still negligible. As is seen in fig. 7 they fluctuate around zero. Martin et al. [10,12] have found a significantly non-zero t_3^4 moment in the $A_2(1310)$ region. This corresponds to the D_{2N} amplitude (NPE D wave with helicitiy m = 2) accounting for ∿ 10% of the D_N amplitude. In our data there is no significant deviation of M > 2 moments from zero except possibly above 1500 MeV. Therefore we proceed exactly as in section 2, fitting m ≤ 1 transversity amplitudes to the high-t moments with M ≤ 2. Again mostly unique solutions have been obtained for the partial-wave intensities. The results are shown in fig. 8.

The intensities of the m = 0 waves are of similar shape to those at low t as described in section 3. We have calculated for each partial wave the ratio of intensity at low t $[0.01 < |t| < 0.20\ (\mathrm{GeV/c})^2]$ to that at high t $[0.20 < |t| < 1.00\ (\mathrm{GeV/c})^2]$. The ratio is $5.3^{+2.1}_{-2.0}$ for the S wave, 3.6 ± 1.4 for the P_0 wave, $7.0^{+1.2}_{-1.0}$ for the D_0 wave and $4.7^{+1.5}_{-1.2}$ for the F_0 wave. These ratios are to be compared with the value of 6-7 calculated by integrating the following "OPE + absorption" formulae over the corresponding t ranges:

$$\frac{d\sigma_0^\ell}{dt} \propto \frac{-t}{(t - \mu^2)^2} e^{A(t-\mu^2)} ,$$

where

σ_0^ℓ is a partial cross-section for the $\pi\pi$ wave with spin ℓ and helicity m = 0,

μ is a pion mass, and

A = 7-7.5 has been taken from the fits to $\pi^+\pi^-$ data of another paper [37].

There is a reasonable agreement with this value. For the P wave the reader is referred to the discussion in section 4.

The UPE m = 1 waves are reduced by a smaller factor (P_U by 4.0 ± 1.2, D_U by $3.1^{+1.1}_{-0.6}$ and F_U by 2.0 ± 0.8) as could be expected from absorption models.

Finally the NPE amplitudes are even less reduced (P_N by 1.7 ± 0.5, D_N by 1.4 ± 0.3 and F_N by 3.5 ± 1.7) except for the badly determined F_N wave. The D_N wave, which is expected to have a significant contribution of A_2(1310) by the ρ exchange, is nearly as strong at high t as the D_0 wave.

7. CONCLUDING REMARKS

Since the polarization effect is small in the reaction $\pi^-p \to K^+K^-n$, one could wonder whether it is worth while to use the whole apparatus of transversity amplitudes. A simple model assuming spin-flip dominance, phase coherence and identical vanishing of M = 2 moments as in ref. [5], seems to be a sufficient tool for an energy-independent partial-wave analysis. This approach has also been tried and led to worse fits. The most interesting feature of these fits is the reappearance of an ambiguity in the S and P waves. The relevant results are shown in fig. 9 together with those of the Argonne group. Let us remember that a similar ambiguity is present in the $\pi^+\pi^-$ studies [6,7] based on similar assumptions. This suggests that such an ambiguity may be inherent in these assumptions. The polarization effect, though not very significant in individual moments, seems to be essential. The use of all the available moments allows us to obtain unique solutions in a completely model-independent fashion. Our approach has obvious limitations. The convenient helicity amplitudes are not available without assumptions on the missing phase between the g and h amplitudes. Also the calculation of phase shifts is impossible without assumptions on the absolute phases. Finally, as we have already mentioned, our estimates of resonance parameters are usually connected with larger errors than those coming from direct fits to moments. On the other hand, our results are free from any uncertainties other than purely experimental ones. Therefore they can serve as a stringent test for all model-dependent studies.

Acknowledgements

The authors are very grateful to Drs. K. Fiałkowski and M.R. Pennington for many helpful suggestions. The discussion with Dr. A.B. Wicklund on the comparison of our data with those of the Argonne group was very useful.

REFERENCES

[1] A.J. Pawlicki et al., Phys. Rev. Lett. 37 (1976) 971.

[2] A.J. Pawlicki et al., Phys. Rev. Lett. 37 (1976) 1666.

[3] A.J. Pawlicki et al., Phys. Rev. D 15 (1977) 3196.

[4] D. Cohen et al., Argonne preprint ANL-HEP-78-22, 1978.

[5] B. Hyams et al., Nucl. Phys. B64 (1973) 134.

[6] B. Hyams et al., Nucl. Phys. B100 (1975) 205.

[7] P. Estabrooks and A.D. Martin, Nucl. Phys. B95 (1975) 322.

[8] H. Becker et al., Tensor meson production in the reaction $\pi^- p \to K^+ K^- n$ (in preparation).

[9] N.M. Cason et al., Phys. Rev. Lett. 36 (1976) 1485.

[10] B. Baldi et al., Phys. Lett. 74B (1978) 413.

[11] A.D. Martin et al., Phys. Lett. 74B (1978) 417.

[12] A.D. Martin et al., Nucl. Phys. B140 (1978) 158.

[13] W. Blum et al., Phys. Lett. 57B (1975) 403.

[14] G. Hentschel, Thesis, Max Planck Institute report MPI-PAE/Exp.El.56, 1976.

[15] J. De Groot, Thesis, Zeeman Laboratory, Amsterdam, 1978.

[16] H. Becker et al., Nucl. Phys. B150 (1979) 301.

[17] H. Becker et al., Nucl. Phys. B151 (1979) 46.

[18] G. Lutz and K. Rybicki, Max Planck Institute report MPI-PAE/Exp.El.75, 1978.

[19] E. Barrelet, Nuovo Cimento 8A (1972) 331.

[20] R.P. Feynman, M. Kislinger and F. Ravndall, Phys. Rev. D 3 (1971) 2706.

[21] A.J. Hey and D. Morgan, Reports on Progress in Physics 41 (1978) 675.

[22] V. Chabaud et al., Nucl. Phys. B145 (1978) 349.

[23] B. Hyams et al., Nucl. Phys. B146 (1978) 303.

[24] A.C. Irving and C. Michael, Nucl. Phys. B82 (1974) 282.

[25] Particle Data Group, Review of Particle Properties, Phys. Lett. 75B (1978).

[26] W. Beusch et al., Phys. Lett. 60B (1975) 101.

[27] W. Wetzel et al., Nucl. Phys. B115 (1976) 208.

[28] V.A. Polychronakos et al., Phys. Rev. D 19 (1979) 1317.

[29] N.P. Samios, M. Goldberg and B.T. Meadows, Rev. Mod. Phys. 46 (1974) 49.

[30] F. Barreiro et al., Nucl. Phys. B121 (1977) 237.

[31] C. Evangelista et al., Nucl. Phys. B127 (1977) 384.

[32] M.J. Corden et al., Nucl. Phys. B157 (1979) 250.

[33] H. Becker et al., Contribution to the 18th Int. Conf. on High-Energy Physics, Tbilisi, 1976.

[34] P.K. Williams, Phys. Rev. D 1 (1970) 1312.

[35] A.D. Martin and M.R. Pennington, Ann. Phys. (USA) 114 (1978) 1.

[36] L. Görlich, Thesis, Institute of Nuclear Physics, Cracow, 1979.

[37] B. Hyams et al., Phys. Lett. 51B (1974) 272.

Table 1

Wave	J^P	I = 0	I = 1
S	0^+	S*(980), ε(1300)	δ(980)
P	1^-	ϕ(1020)	ρ(770)
D	2^+	f(1270), f′(1515)	A_2(1310)
F	3^-	ω(1670)	g(1690)

Table 2

ℓ_{max}	2	3
m_{KK} (MeV)	1100-1460	1460-1740
No. of amplitudes ($m \leq 1$)	14	20
No. of real parameters ($m \leq 1$)	26	38
No. of moments ($M \leq 2$)	31	47
$\langle \chi^2/d.f. \rangle$	0.9	1.5

Table 3

Wave	S	P	D	F
Resonance R	ε(1300)	ρ(770) tail	f(1270)	g(1690)
Mass range (MeV)	1100-1420	1100-1420	1100-1660	1460-1740
BR($\bar{K}K/\pi\pi$)	$0.068^{+0.017}_{-0.021}$	$0.081^{+0.029}_{-0.025}$	$0.069^{+0.023}_{-0.031}$	$0.191^{+0.040}_{-0.037}$
FKR model [20,21]	0.237	-	0.058	0.180
$x(R \to \bar{K}K)$ (%)	$6.4^{+1.6}_{-2.0}$	-	$5.8^{+1.9}_{-2.6}$	$4.9^{+1.1}_{-1.0}$

Table 4

	Fit 1	Fit 2	Fit 3
α_f^{KK} ($\sqrt{\mu b/GeV}$)	$0.115\ ^{+\,0.019}_{-\,0.026}$	0.128 ± 0.018	$0.126\ ^{+\,0.010}_{-\,0.029}$
$\alpha_{A_2}^{KK}$ ($\sqrt{\mu b/GeV}$)	0.010 ± 0.008	0.021 ± 0.006	0 (fixed)
$\alpha_{f'}^{KK}$ ($\sqrt{\mu b/GeV}$)	$0.071\ ^{+\,0.093}_{-\,0.017}$	$0.129\ ^{+\,0.010}_{-\,0.017}$	0.137 ± 0.033
$m_{f'}$ (MeV)	1492 ± 29	1516 } fixed	1478 ± 21
$\Gamma_{f'}$ (MeV)	$150\ ^{+\,83}_{-\,50}$	65 } fixed	$164\ ^{+\,52}_{-\,43}$
ϕ_A (°)	$-(78 \pm 23)$	$-(80\ ^{+\,22}_{-\,18})$	-
$\phi_{f'}$(°)	(163 ± 20)	(204 ± 7)	$(206\ ^{+\,9}_{-\,61})$
$x(f' \to \pi\pi)$ (%)	$(2.7\ ^{+\,7.1}_{-\,1.3})$	$(8.9\ ^{+\,3.3}_{-\,3.8})$	(10.1 ± 4.9)
χ^2/NDF	1.5/7	5.1/9	2.2/9

Table 5

Ref.	Reaction	Plab (GeV/c)	Mass (MeV)	Width (MeV)	$x(f' \to \pi\pi)$ (%)
[26,27]	$\pi^- p \to K_S^0 K_S^0 n$	8.9	-	-	≤ 0.9
[28]	$\pi^- p \to K_S^0 K_S^0 n$	6.7	-	$92\ ^{+\,39}_{-\,22}$	-
[30]	$K^- p \to K_S^0 K_S^0 \Lambda^0 (\Sigma^0)$	4.2	1522 ± 6	$62\ ^{+\,19}_{-\,14}$	3.0
[31]	$K^- p \to K^+ K^- \Lambda^0 (\Sigma^0)$	10.0	1528 ± 7	72 ± 25	-
[3]	$\pi^- p \to K^+ K^- n$ and $\pi^+ n \to K^+ K^- p$	6.0	1506 ± 5	66 ± 10	1.2 ± 0.4
[32]	$\pi^- p \to \pi^+ \pi^- n$	12.0, 15.0	1502 ± 25	165 ± 42	19 ± 3
This work	$\pi^- p \to K^+ K^- n$	17.2, 18.4	1492 ± 29	$150\ ^{+\,83}_{-\,50}$	$2.7\ ^{+\,7.1}_{-\,2.3}$

Figure captions

Fig. 1 : The K^+K^- effective mass spectrum and moments of the angular distribution for low four-momentum transfer [$0.01 < |t| < 0.20$ $(GeV/c)^2$]. The moments are normalized in such a way that $t_0^0 = 1/\sqrt{4\pi}$. The p_M^L moments for the $\pi^+\pi^-$ results [18] are shown as full lines. Open circles in the mass distribution show the raw data.

Fig. 2 : Partial-wave intensities at low t. $|S|^2$ represents the S-wave cross-section in microbarns for the t bin from 0.01 to 0.20 $(GeV/c)^2$ in Δm = 40 MeV mass bins. Full circles denote the solutions which are unique or, in cases of ambiguity, more likely from the point of view of continuity of results, open circles denote possible other solutions. The curves on the $|D_0|^2$ and $|F_0|^2$ show the results of the fits described in the text. The curve on the $|P_0|^2$ represents the SU(3) prediction of the ρ-meson tail decaying into K^+K^-.

Fig. 3 : The ratio of transversity amplitudes for the D and F waves at low t. The dashed line shows the OPE prediction, the full line the ratio $|g_0^D|/|h_0^D|$ for $\pi^+\pi^-$ [17].

Fig. 4 : The ratios $|P_U|/(\sqrt{2}|P_0|)$, $|D_U|/(\sqrt{6}|D_0|)$ and $|F_U|/(\sqrt{12}|F_0|)$ versus K^+K^- effective mass at low t. Only values with errors below 100% are plotted. The shaded area shows the trend of the $\pi^+\pi^-$ results from ref. [17].

Fig. 5 : Relative phases of the transversity amplitudes at low t below 1500 MeV.

Fig. 6 : The Barrelet zeros of the K^+K^- transversity amplitudes (g in fig. 6a, h in fig. 6b) at low t. The real parts are represented by squares, the imaginary ones by circles. Full lines show the $\pi^+\pi^-$ results from ref. [17].

Fig. 7 : The K^+K^- effective mass distribution and normalized moments for high t [$0.20 < |t| < 1.0$ $(GeV/c)^2$].

Fig. 8 : Partial-wave intensities at high t. Units and conventions are as in fig. 2.

Fig. 9 : Partial-wave intensities at low t calculated using the model assumptions (see text). Two solutions are denoted by full circles and squares. The results of the Argonne group [4] are shown as open circles and triangles. They have been normalized to our solution by demanding the same integrated intensity of the D_0 wave.

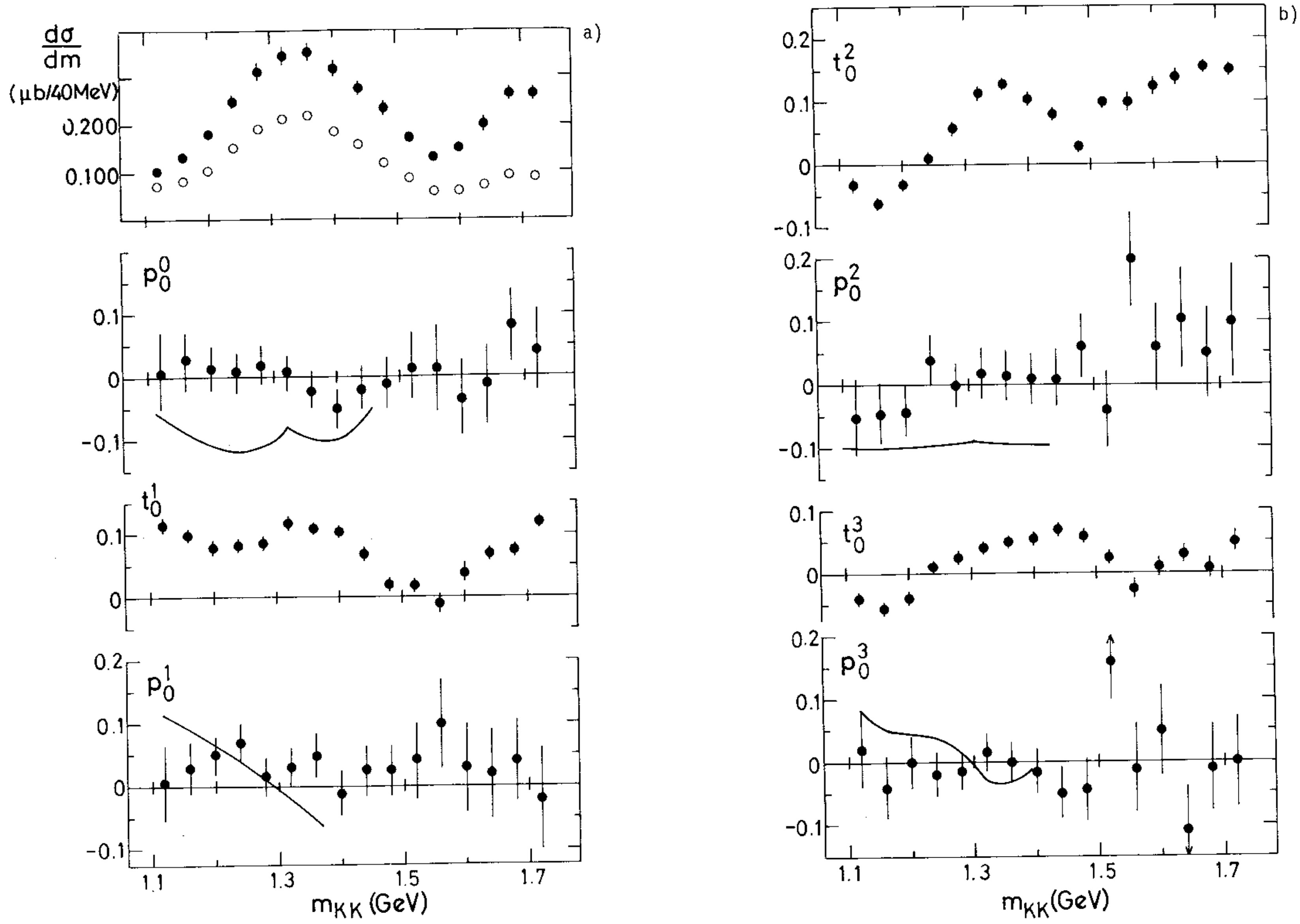

a)
b)
dσ/dm
(μb/40MeV)
0.200
0.100
p_0^0
t_0^1
p_0^1
t_0^2
p_0^2
t_0^3
p_0^3
0.2
0.1
0
-0.1
1.1
1.3
1.5
1.7
m_{KK} (GeV)

Fig. 1 a) b)

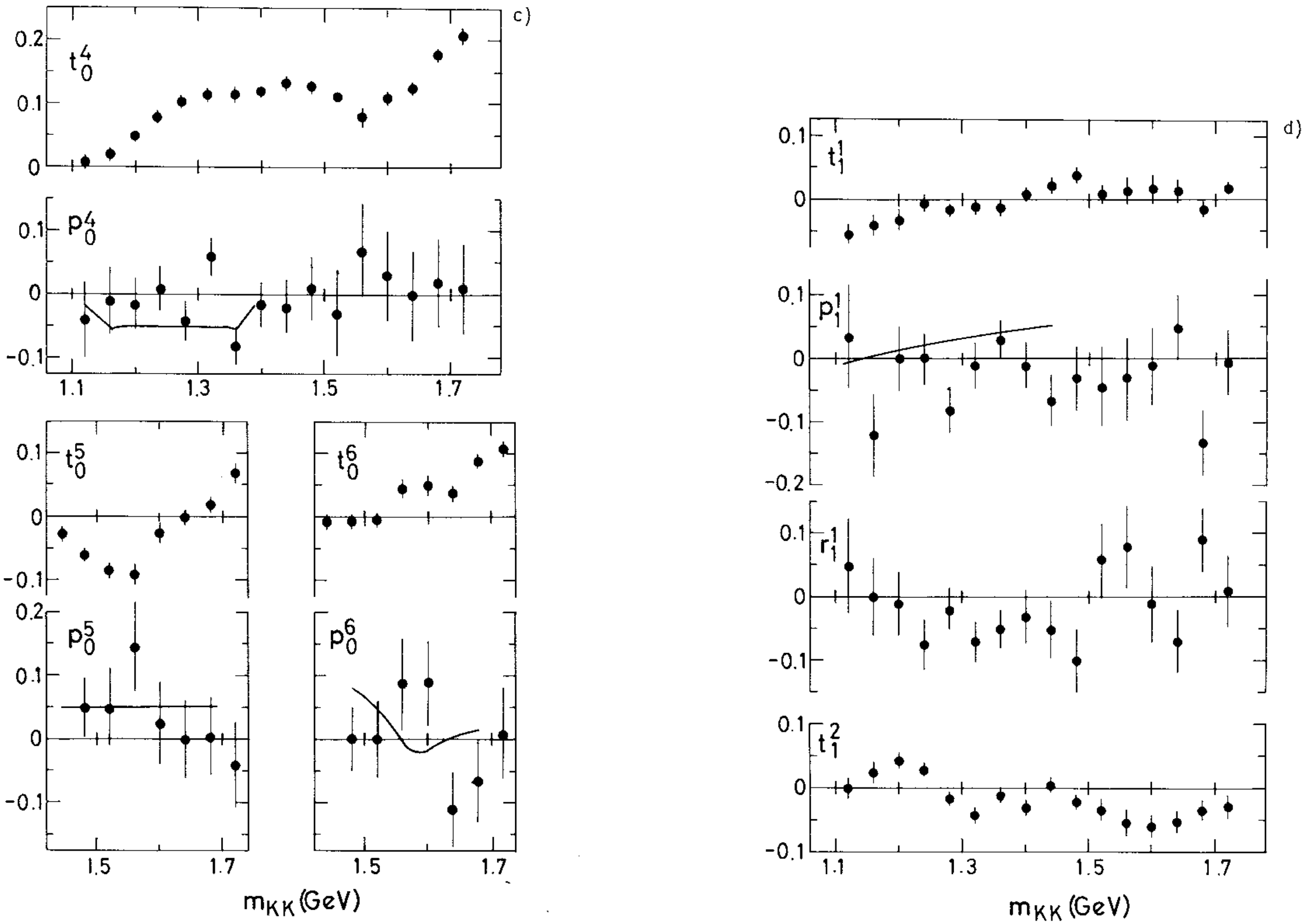

Fig. 1 c) d)

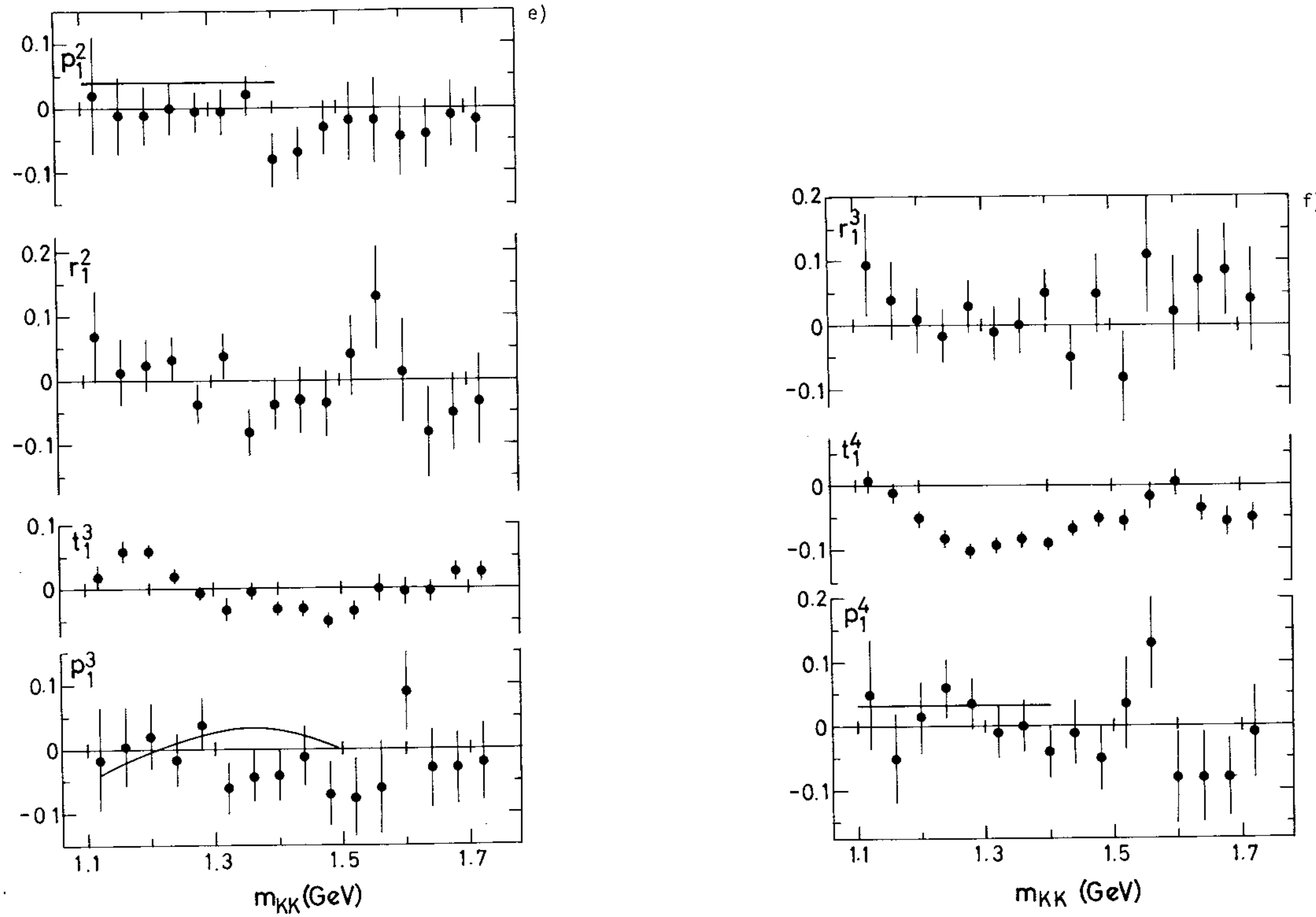

Fig. 1 e) f)

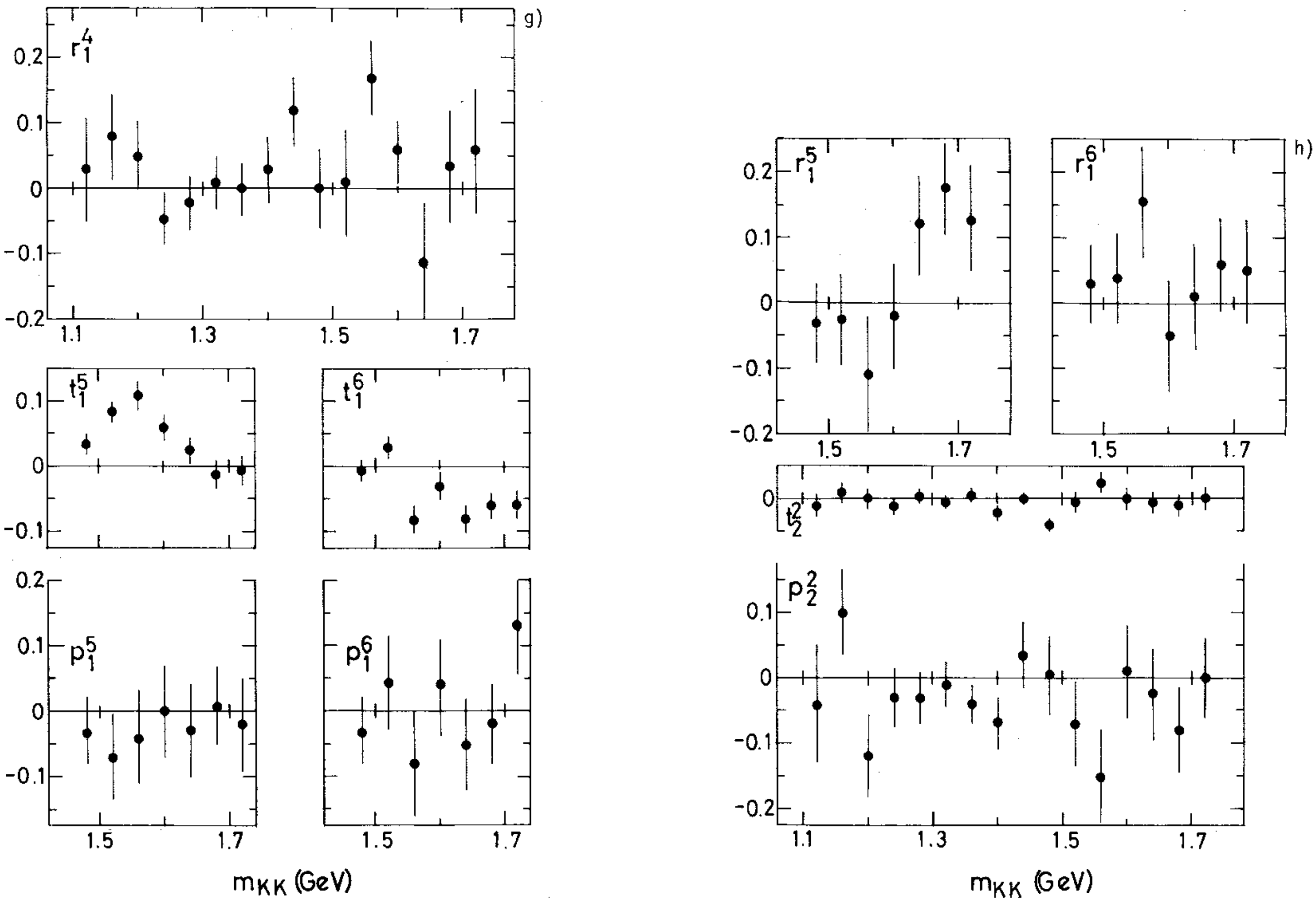

Fig. 1 g) h)

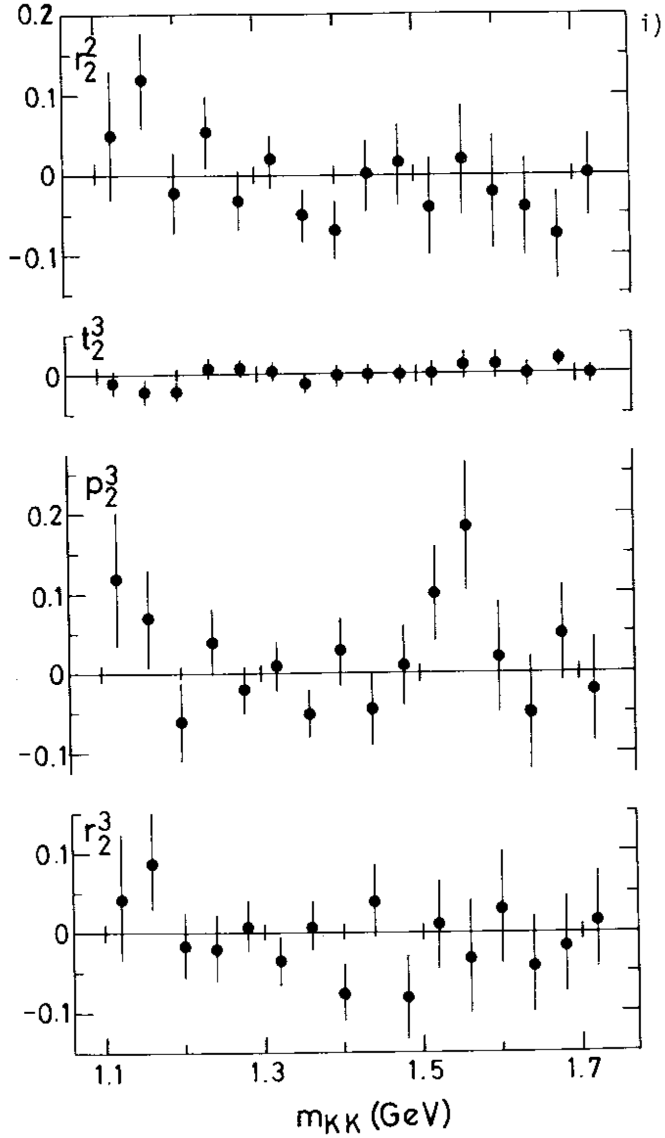
i)
r_2^2
t_2^3
p_2^3
r_2^3
0.2
0.1
0
-0.1
1.1
1.3
1.5
1.7
m_{KK} (GeV)

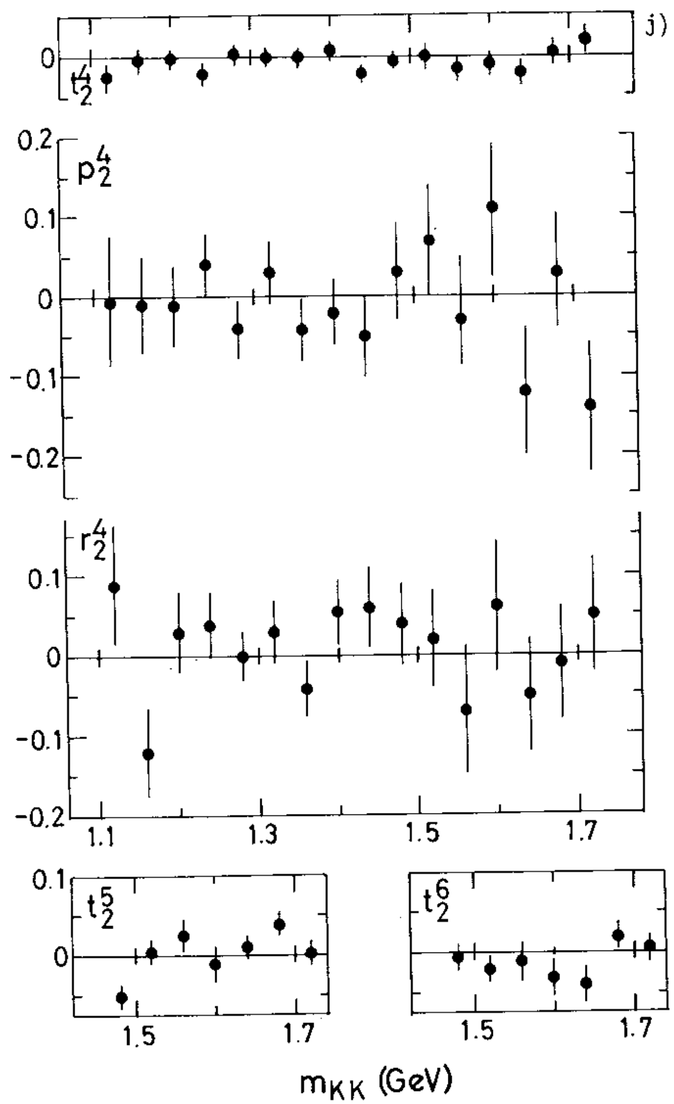
j)
t_2^4
p_2^4
r_2^4
t_2^5
t_2^6
0.2
0.1
0
-0.1
-0.2
1.1
1.3
1.5
1.7
m_{KK} (GeV)

Fig. 1 i) j)

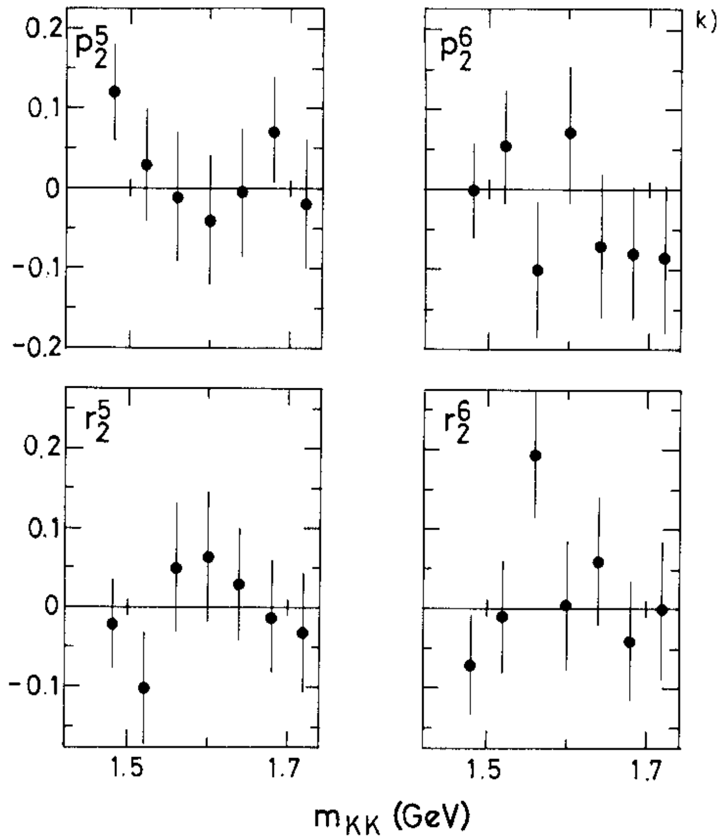

Fig. 1 k)

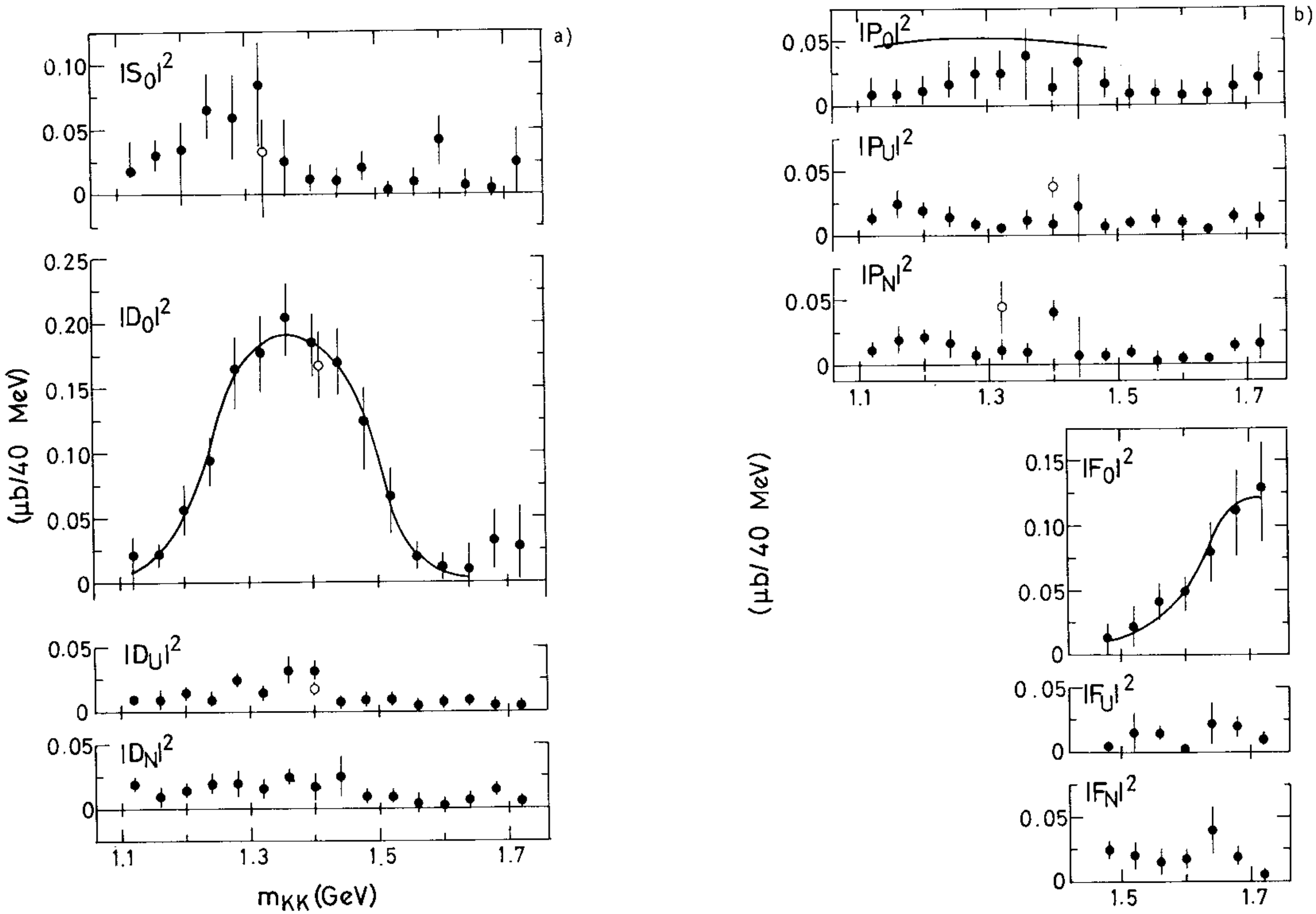
a)
b)
$|S_0|^2$
$|D_0|^2$
$|D_U|^2$
$|D_N|^2$
$|P_0|^2$
$|P_U|^2$
$|P_N|^2$
$|F_0|^2$
$|F_U|^2$
$|F_N|^2$
(μb/40 MeV)
m_{KK} (GeV)
0.10
0.05
0
0.25
0.20
0.15
1.1
1.3
1.5
1.7

Fig. 2

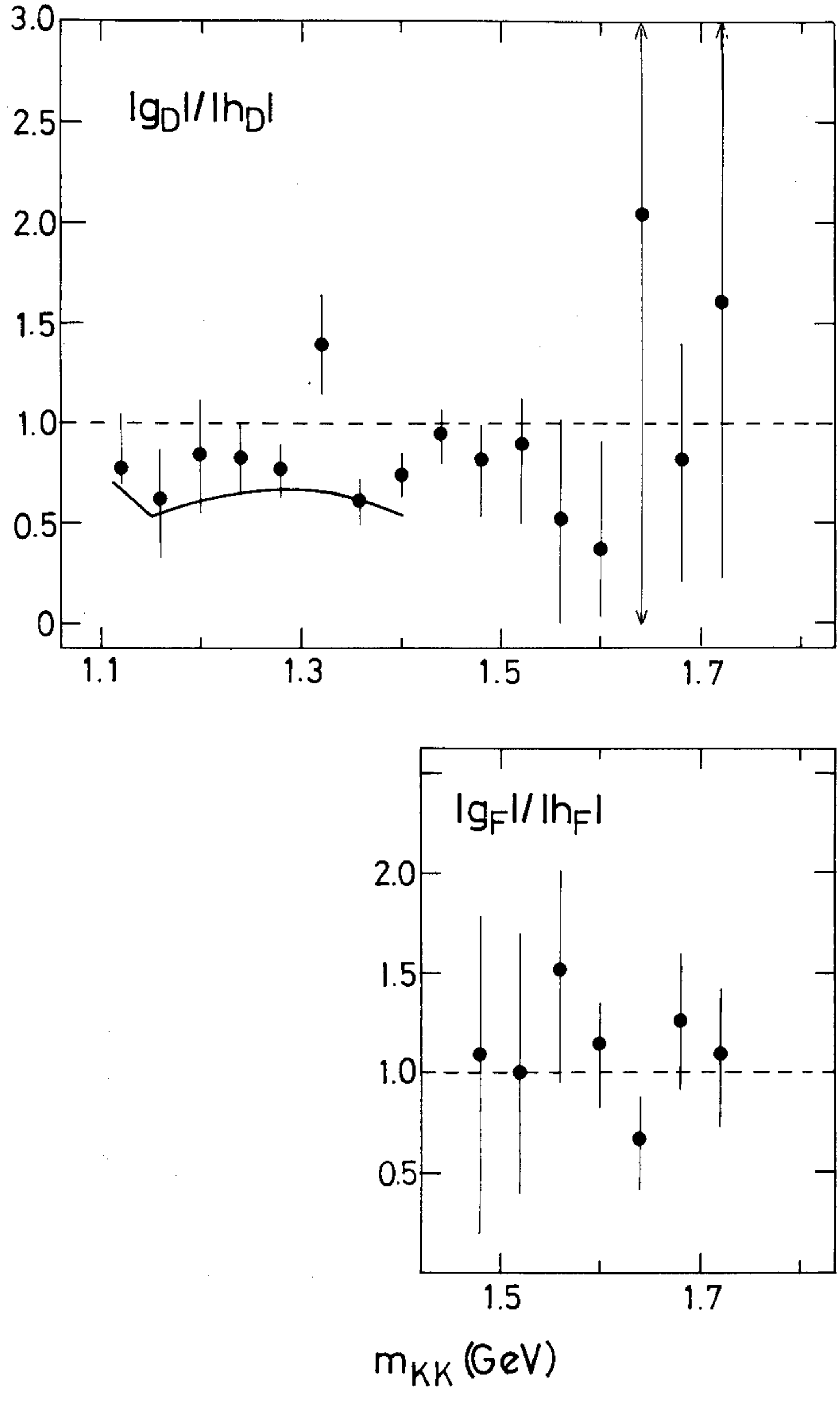

Fig. 3

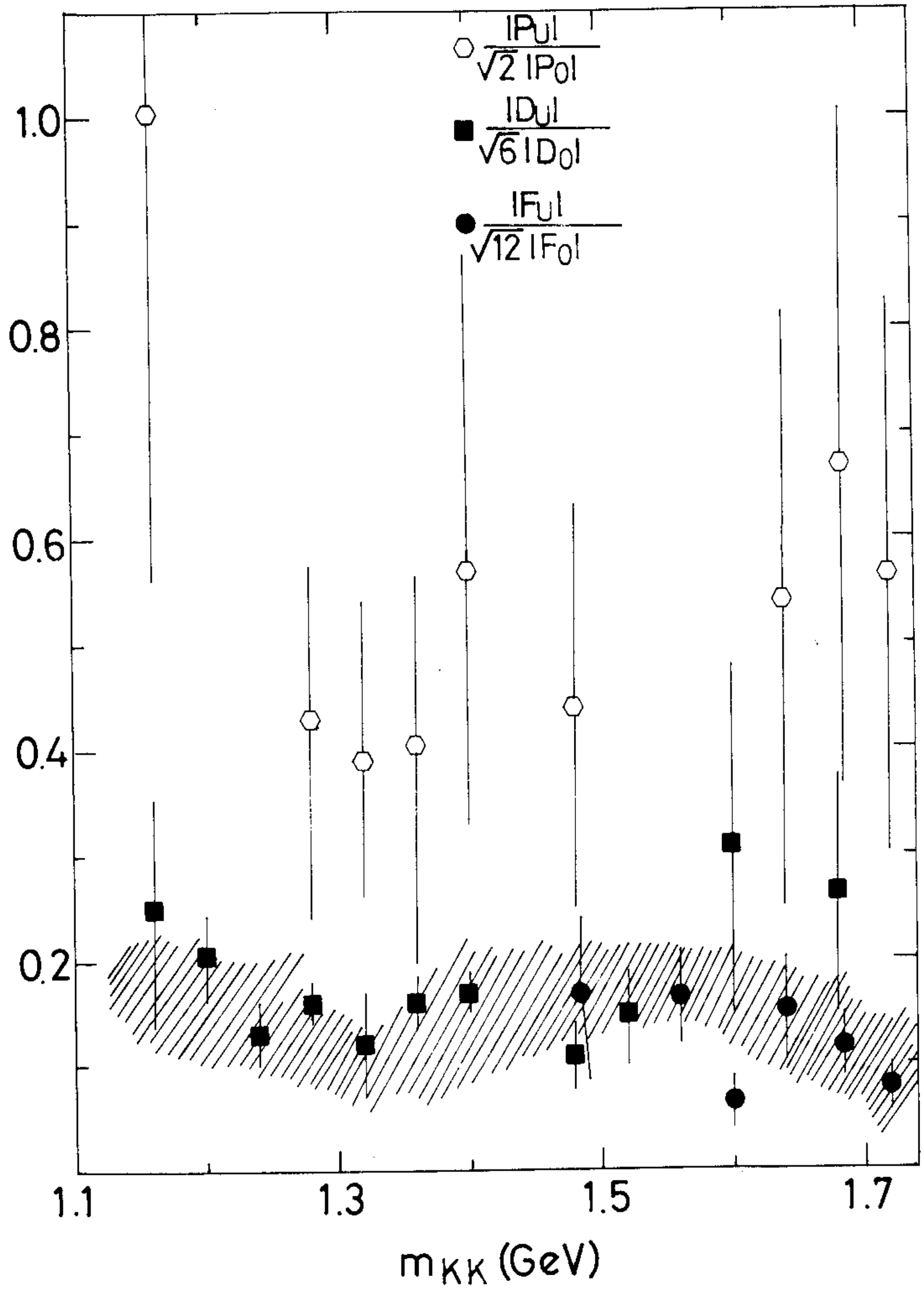

$\frac{|P_U|}{\sqrt{2}|P_0|}$
$\frac{|D_U|}{\sqrt{6}|D_0|}$
$\frac{|F_U|}{\sqrt{12}|F_0|}$
1.0
0.8
0.6
0.4
0.2
1.1
1.3
1.5
1.7
m_{KK} (GeV)

Fig. 4

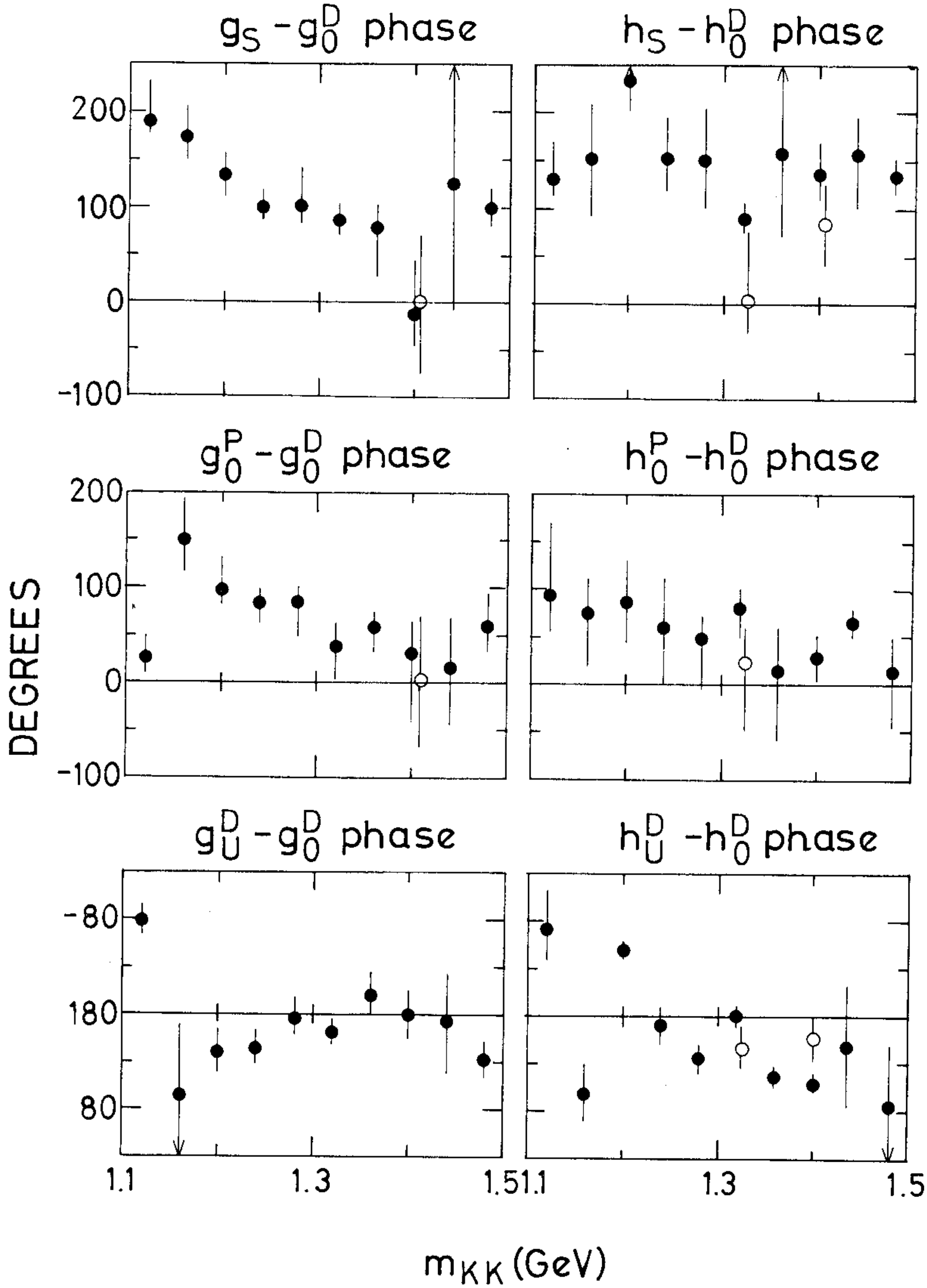

$g_S - g_0^D$ phase
$h_S - h_0^D$ phase
$g_0^P - g_0^D$ phase
$h_0^P - h_0^D$ phase
$g_U^D - g_0^D$ phase
$h_U^D - h_0^D$ phase
DEGREES
200
100
0
-100
-80
180
80
1.1
1.3
1.5
m_{KK} (GeV)

Fig. 5

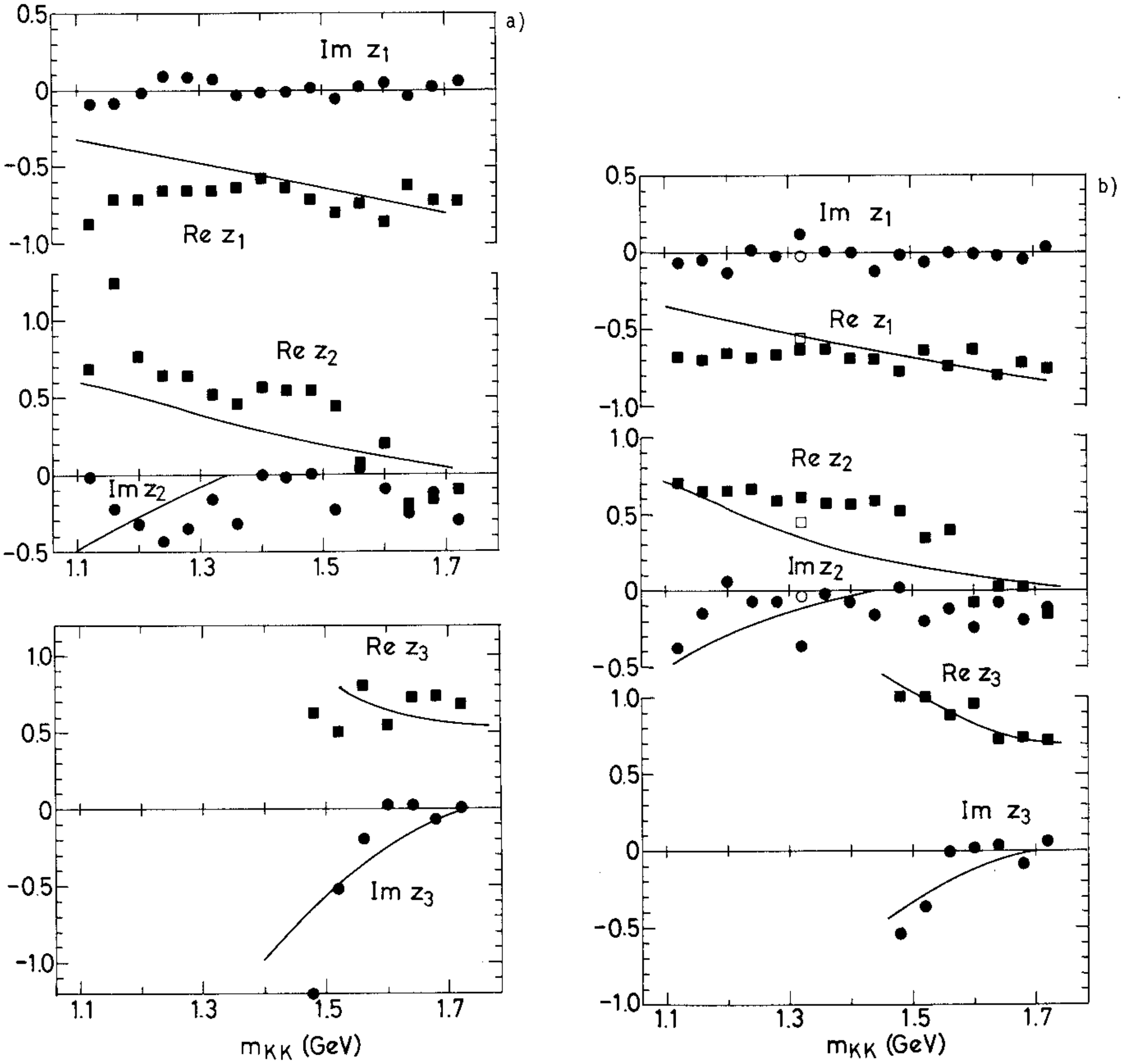

a)
Im z_1
Re z_1
Re z_2
Im z_2
Re z_3
Im z_3
m_{KK} (GeV)
b)
Im z_1
Re z_1
Re z_2
Im z_2
Re z_3
Im z_3
m_{KK} (GeV)

Fig. 6

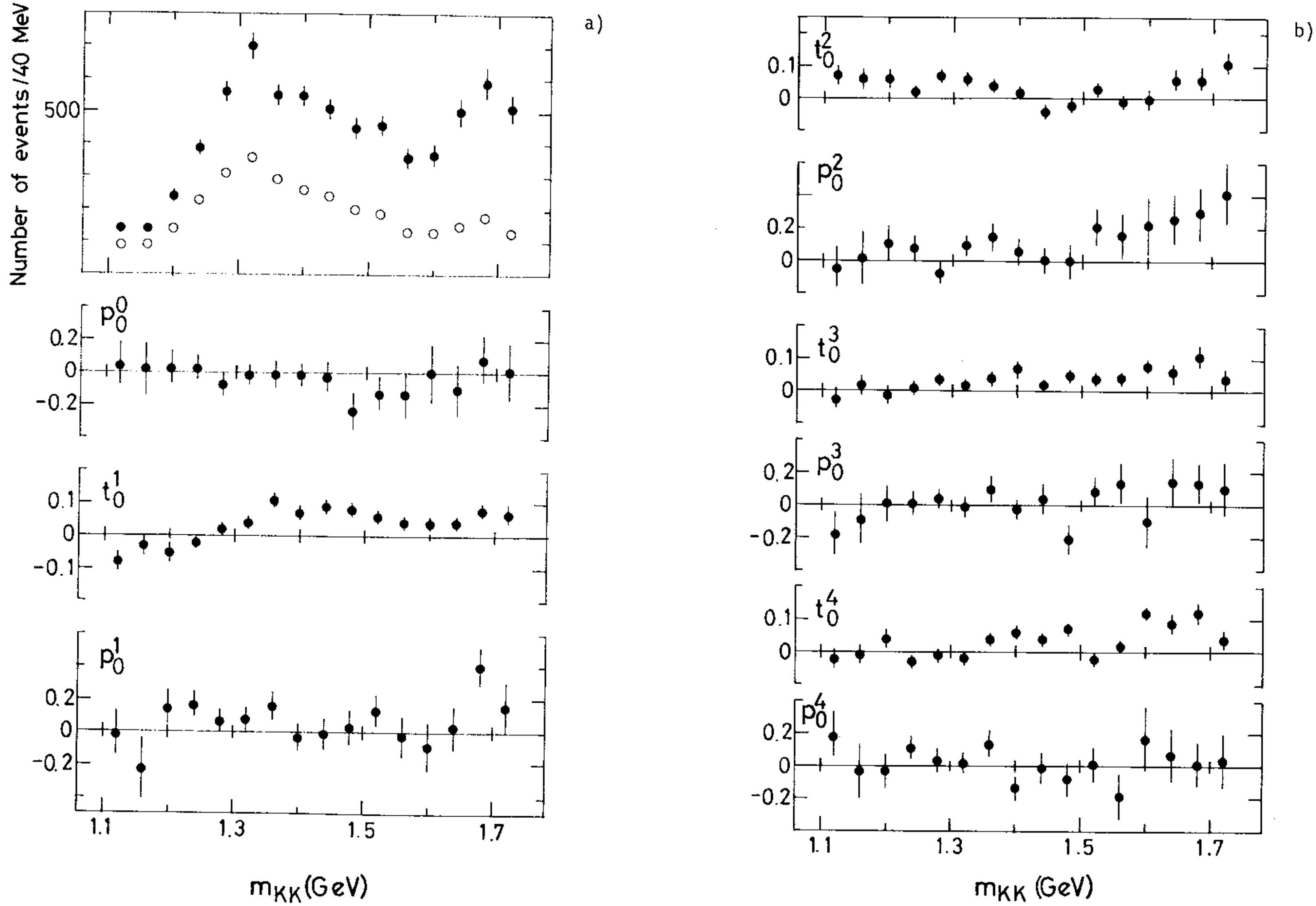
a)
Number of events/40 MeV
500
p$_0^0$
t$_0^1$
p$_0^1$
0.2
0
-0.2
0.1
-0.1
1.1
1.3
1.5
1.7
m$_{KK}$(GeV)
b)
t$_0^2$
p$_0^2$
t$_0^3$
p$_0^3$
t$_0^4$
p$_0^4$
m$_{KK}$ (GeV)

Fig. 7 a) b)

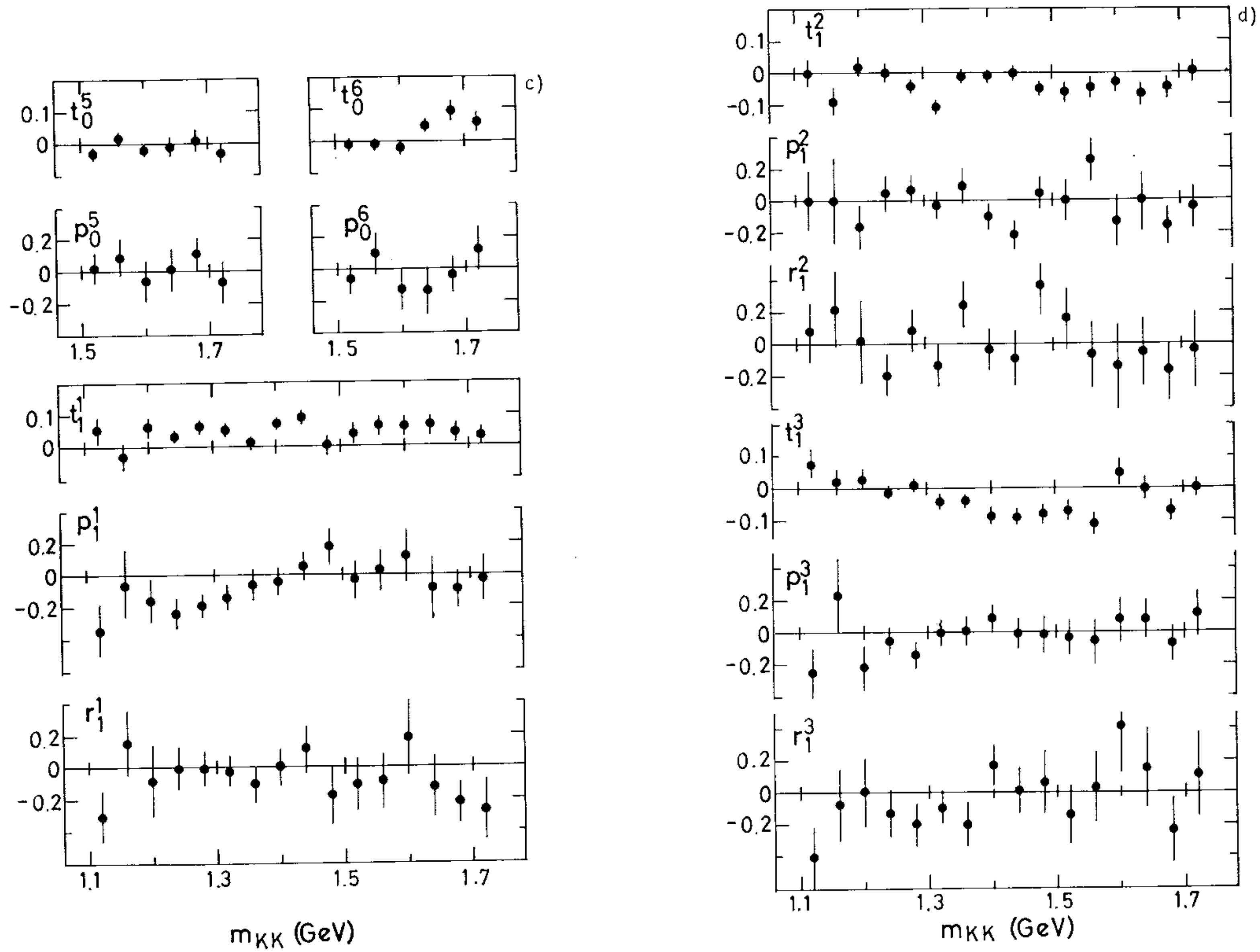

Fig. 7 c) d)

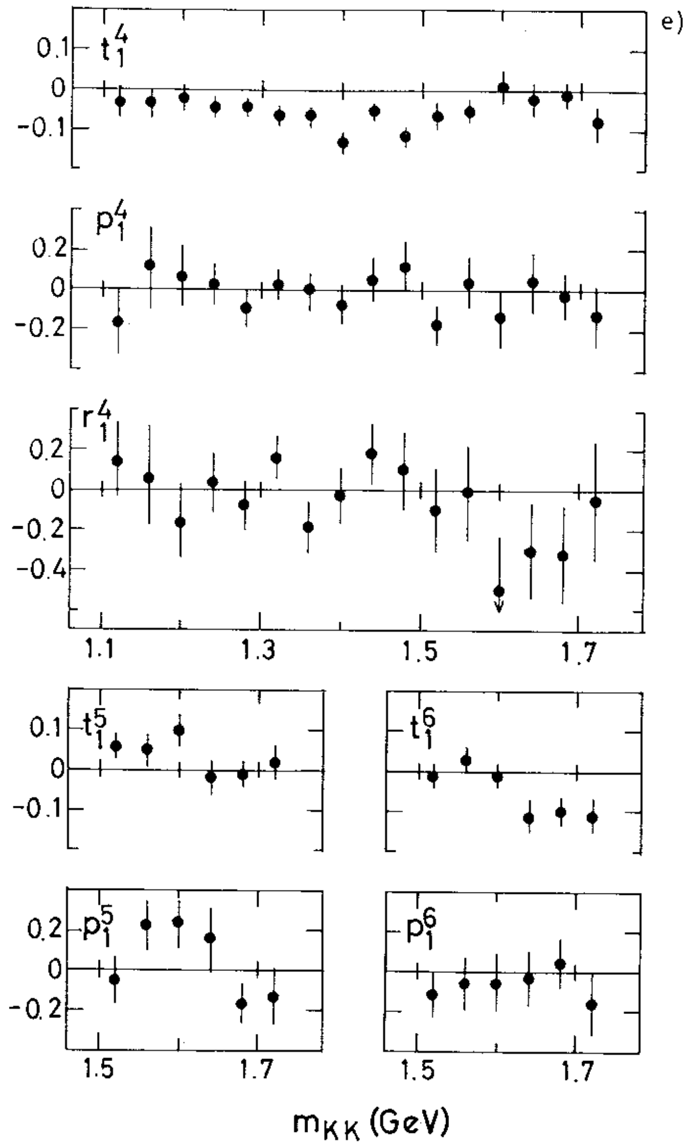
e)
t_1^4
p_1^4
r_1^4
t_1^5
t_1^6
p_1^5
p_1^6
m_{KK} (GeV)

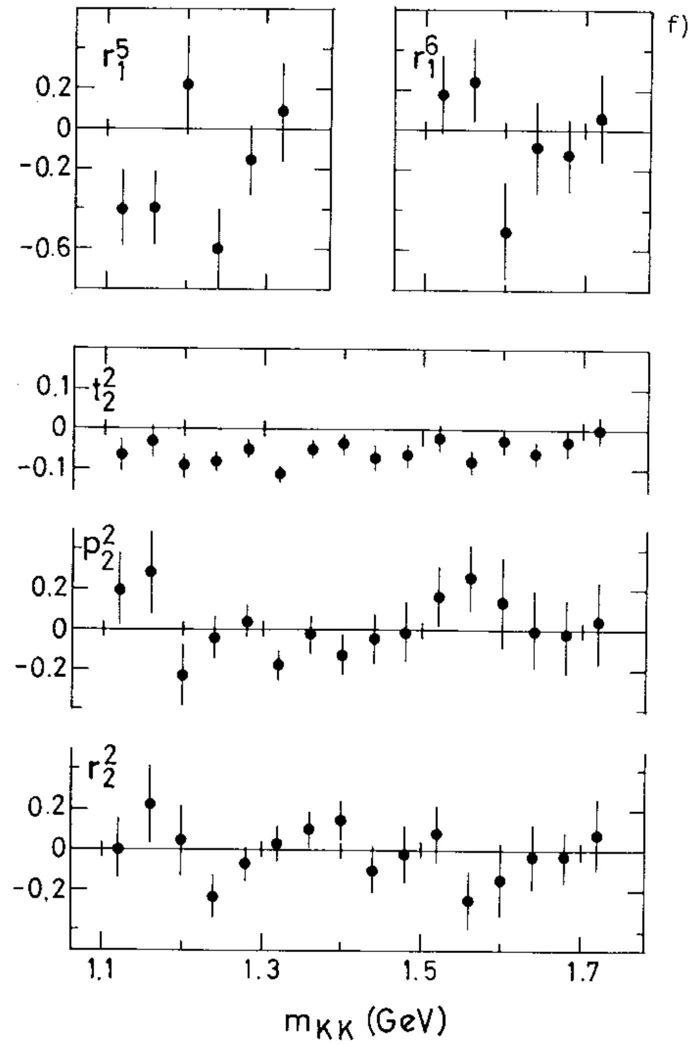
f)
r_1^5
r_1^6
t_2^2
p_2^2
r_2^2
m_{KK} (GeV)

Fig. 7 e) f)

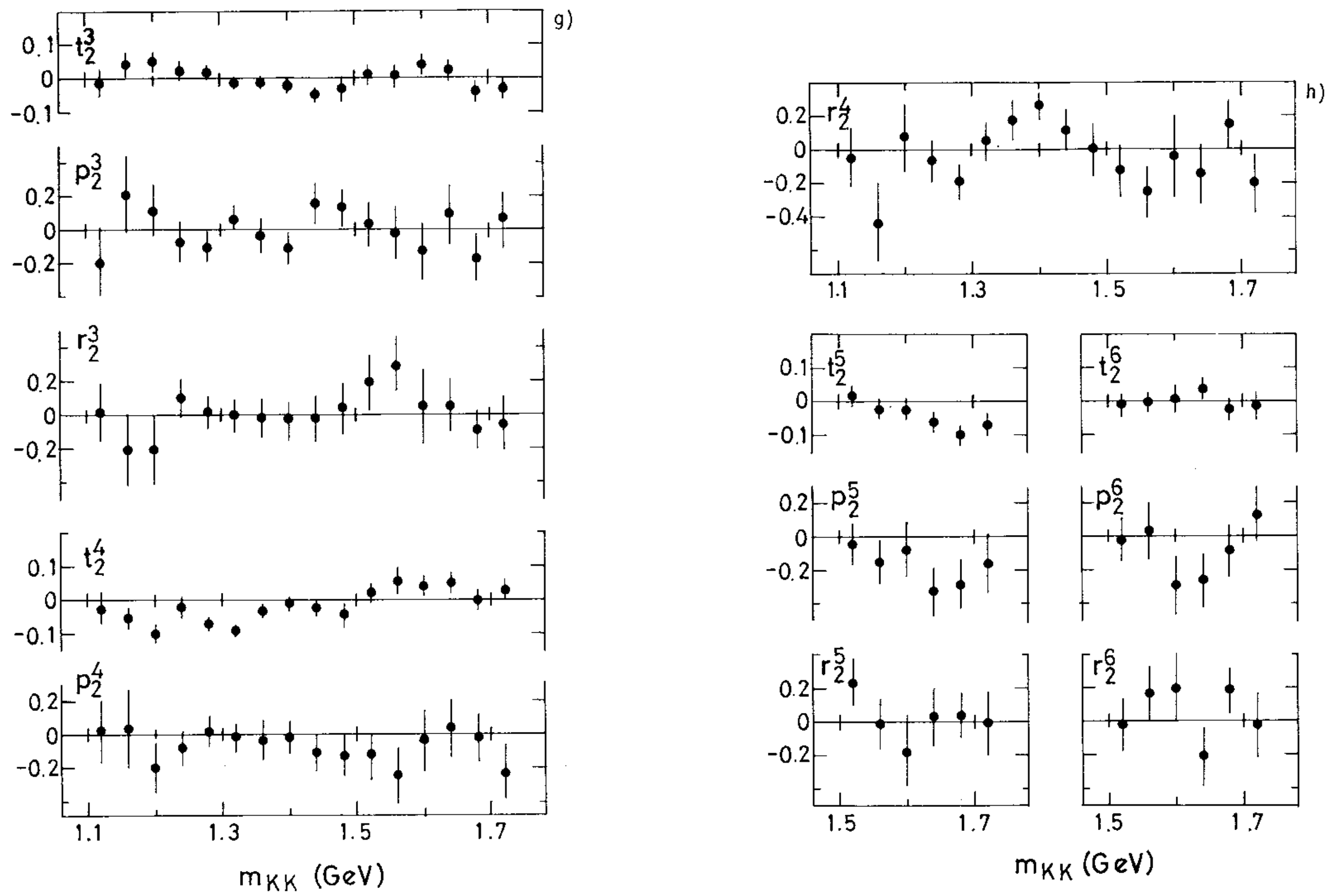

g)
h)
t_2^3
p_2^3
r_2^3
t_2^4
p_2^4
r_2^4
t_2^5
t_2^6
p_2^5
p_2^6
r_2^5
r_2^6
0.1
0
-0.1
0.2
-0.2
-0.4
1.1
1.3
1.5
1.7
m_{KK} (GeV)

Fig. 7 g) h)

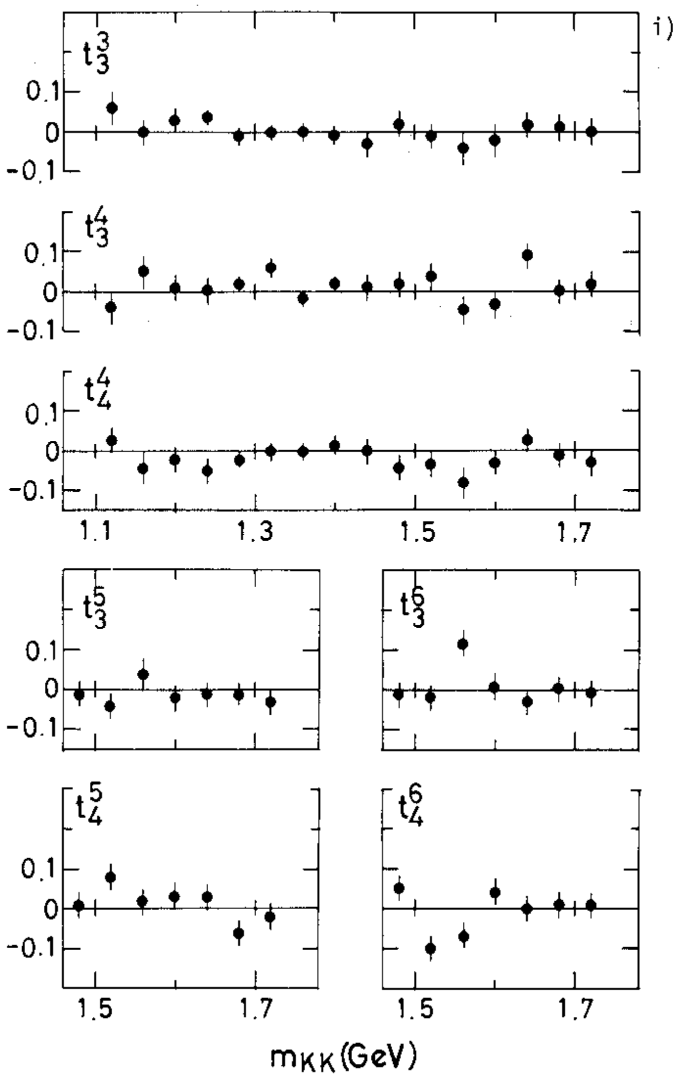

Fig. 7 i)

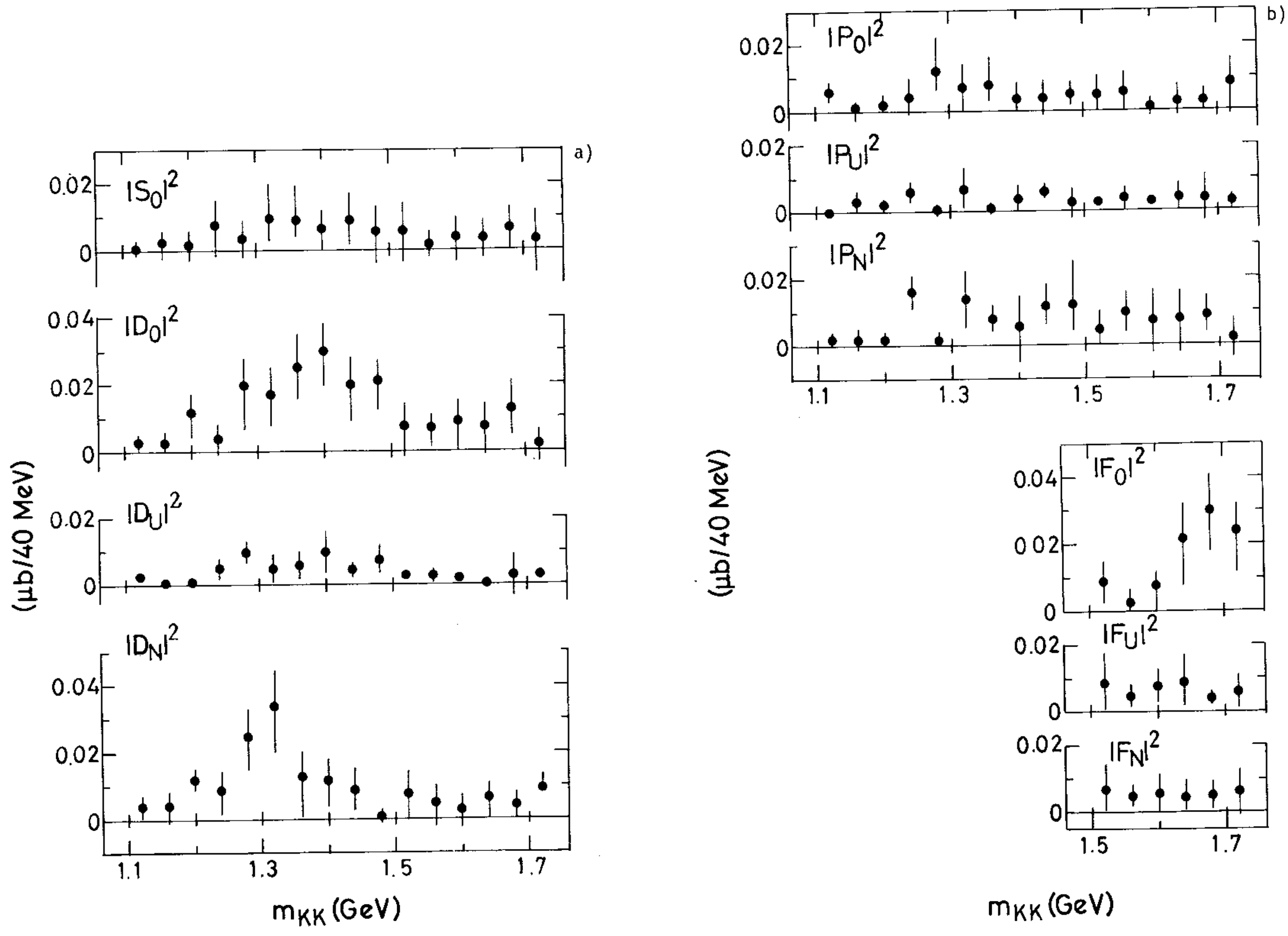

Fig. 8

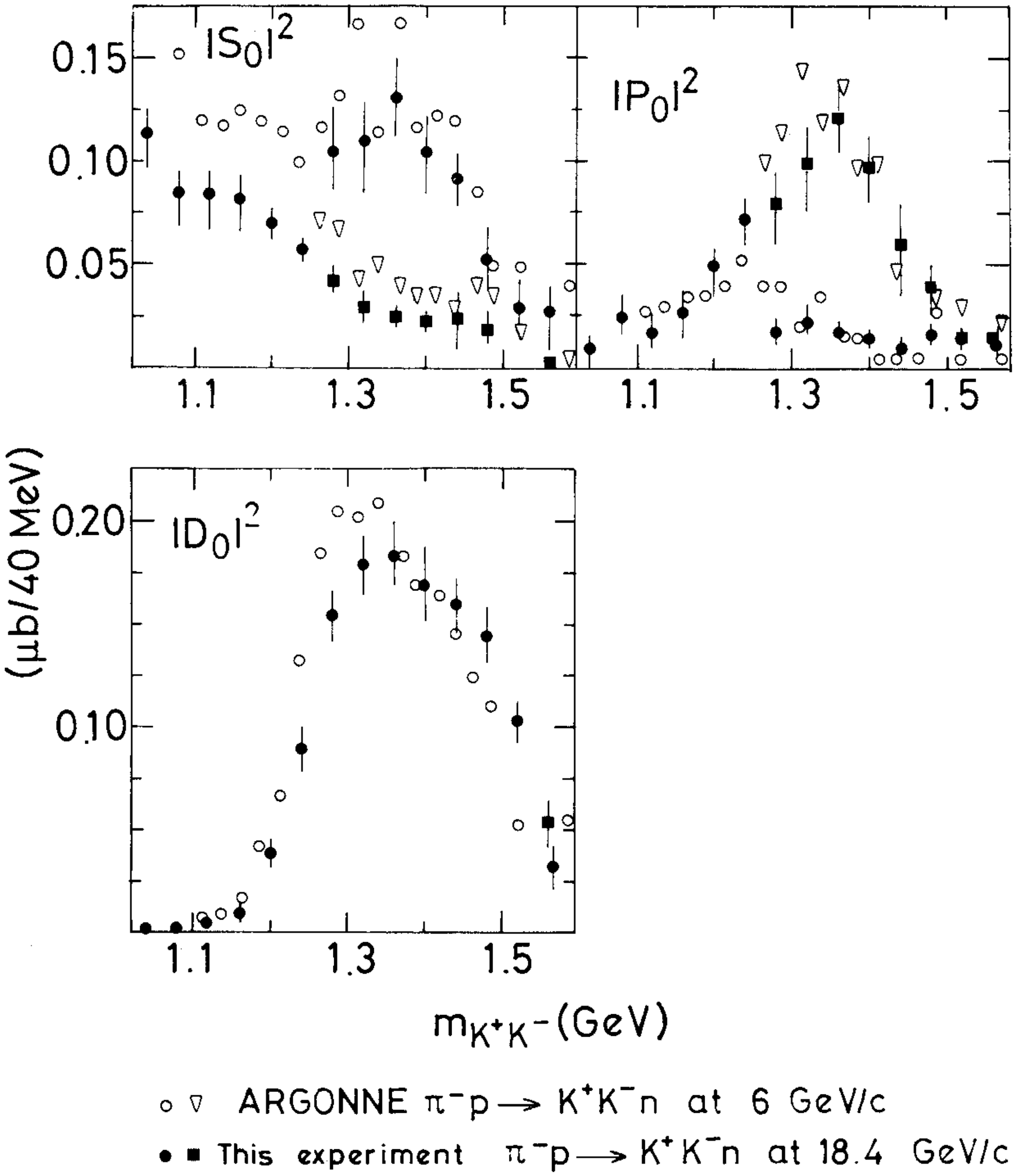

$|S_0|^2$
$|P_0|^2$
$|D_0|^2$
0.15
0.10
0.05
0.20
0.10
1.1
1.3
1.5
(μb/40 MeV)
$m_{K^+K^-}$ (GeV)
○ ▽ ARGONNE $\pi^-p \rightarrow K^+K^-n$ at 6 GeV/c
● ■ This experiment $\pi^-p \rightarrow K^+K^-n$ at 18.4 GeV/c

Fig. 9